DTIC FILE COPY

(2)

AD-A232 377

TECHNICAL REPORT RD-GC-90-10

ANALYSIS OF THE FLUTTER CHARACTERISTICS OF THE ADVANCED KINETIC ENERGY MISSILE (AdKEM) CONTROL SURFACE

Stephen C. Cayson
Roger P. Berry
Guidance and Control Directorate
Research, Development, and Engineering Center

February 1991

U.S. ARMY MISSILE COMMAND
Redstone Arsenal, Alabama 35898-5000

Approved for public release; distribution unlimited.

DESTRUCTION NOTICE

FOR CLASSIFIED DOCUMENTS, FOLLOW THE PROCEDURES IN DoD 5200.22-M, INDUSTRIAL SECURITY MANUAL, SECTION II-19 OR DoD 5200.1-R, INFORMATION SECURITY PROGRAM REGULATION, CHAPTER IX. FOR UNCLASSIFIED, LIMITED DOCUMENTS, DESTROY BY ANY METHOD THAT WILL PREVENT DISCLOSURE OF CONTENTS OR RECONSTRUCTION OF THE DOCUMENT.

DISCLAIMER

THE FINDINGS IN THIS REPORT ARE NOT TO BE CONSTRUED AS AN OFFICIAL DEPARTMENT OF THE ARMY POSITION UNLESS SO DESIGNATED BY OTHER AUTHORIZED DOCUMENTS.

TRADE NAMES

USE OF TRADE NAMES OR MANUFACTURERS IN THIS REPORT DOES NOT CONSTITUTE AN OFFICIAL ENDORSEMENT OR APPROVAL OF THE USE OF SUCH COMMERCIAL HARDWARE OR SOFTWARE.

UNCLASSIFIED

SECURITY CLASSIFICATION OF THIS PAGE

REPORT DOCUMENTATION PAGE

Form Approved
OMB No 0704-0188
Exp. Date: Jun 30, 1986

1a. REPORT SECURITY CLASSIFICATION: UNCLASSIFIED	1b. RESTRICTIVE MARKINGS
2a. SECURITY CLASSIFICATION AUTHORITY	3. DISTRIBUTION/AVAILABILITY OF REPORT: Approved for public release: distribution is unlimited
2b. DECLASSIFICATION/DOWNGRADING SCHEDULE	
4. PERFORMING ORGANIZATION REPORT NUMBER(S): TR-RD-GC-90-10	5. MONITORING ORGANIZATION REPORT NUMBER(S)
6a. NAME OF PERFORMING ORGANIZATION: Guidance & control Dir, RD & E Center, USAMICOM; 6b. OFFICE SYMBOL (If applicable): AMSMI-RD-GC-C	7a. NAME OF MONITORING ORGANIZATION
6c. ADDRESS (City, State, and ZIP Code): Commander, USAMICOM, ATTN: AMSMI-RD-GC-C, RSA, AL 35898-5254	7b. ADDRESS (City, State, and ZIP Code)
8a. NAME OF FUNDING/SPONSORING ORGANIZATION; 8b. OFFICE SYMBOL (If applicable)	9. PROCUREMENT INSTRUMENT IDENTIFICATION NUMBER
8c. ADDRESS (City, State, and ZIP Code)	10. SOURCE OF FUNDING NUMBERS: PROGRAM ELEMENT NO. / PROJECT NO. / TASK NO. / WORK UNIT ACCESSION NO

11. TITLE (Include Security Classification)
Analysis of the Flutter Characteristics of the Advanced Kinetic Energy Missile (AdKEM) Control Surface (UNCL)

12. PERSONAL AUTHOR(S)
Cayson, Stephen C. and Berry, Roger P.

13a. TYPE OF REPORT	13b. TIME COVERED	14. DATE OF REPORT (Year, Month, Day)	15. PAGE COUNT
Final	FROM OCT 89 TO FEB 90	90 August	66

16. SUPPLEMENTARY NOTATION

17. COSATI CODES			18. SUBJECT TERMS (Continue on reverse if necessary and identify by block number)
FIELD	GROUP	SUB-GROUP	Missile Control Fin Flutter, Fin Bending Stiffness, Actuator Dynamic Stiffness

19. ABSTRACT (Continue on reverse if necessary and identify by block number)

This report describes the analysis of the flutter characteristics of the control fin for the Advanced Kinetic Energy Missile (AdKEM). First of all, the control fin stability equation is detemined from the two-degree-of-freedom equations of motion for the fin. This equation is a function of the fin bending stiffness and the actuator dynamic stiffness, which are then found. The fin bending stiffness is found by assuming that there is a distributed load on the fin and solving for the bending moment and angular deflection using numerical intergration. The actuator dynamic stiffness is solved for by applying a torque disturbance to the second order actuator equation of motion and calculating the resulting fin angular deflection. This data is then compared to the existing third order model and non-linear model data to check for validity. Knowing these values, the possibility of fin flutter may be determined.

20. DISTRIBUTION/AVAILABILITY OF ABSTRACT: ☒ UNCLASSIFIED/UNLIMITED ☐ SAME AS RPT. ☐ DTIC USERS	21. ABSTRACT SECURITY CLASSIFICATION: UNCLASSIFIED
22a. NAME OF RESPONSIBLE INDIVIDUAL: Stephen C. Cayson	22b. TELEPHONE (Include Area Code): (205) 876-7626; 22c. OFFICE SYMBOL: AMSMI-RD-GC-C

DD FORM 1473, 84 MAR — 83 APR edition may be used until exhausted. All other editions are obsolete.

SECURITY CLASSIFICATION OF THIS PAGE
UNCLASSIFIED

TABLE OF CONTENTS

		Page
LIST OF ILLUSTRATIONS		iv
1.0	INTRODUCTION	1
2.0	FIN STABILITY EQUATION	2
3.0	CONTROL FIN BENDING STIFFNESS	4
4.0	ACTUATOR DYNAMIC STIFFNESS	6
5.0	CONCLUSIONS AND RECOMMENDATIONS	10
NOMENCLATURE		31
REFERENCES		33
APPENDIX A	TWO DEGREE OF FREEDOM HIGH SPEED FLUTTER MODEL and ARAP SIMPLIFIED CRITERION REPORTS	A–1
APPENDIX B	STABILITY EQUATION PROGRAM LISTING	B–1
APPENDIX C	FIN MOMENT OF INERTIA EQUATIONS DEVELOPMENT	C–1
APPENDIX D	BENDING PROGRAM LISTING	D–1

LIST OF ILLUSTRATIONS

Figure		Page
2–1.	Two–Degree–of–Freedom Control Fin.	11
2–2.	AdKEM Control Fin.	12
2–3.	AdKEM Control Fin Stability Regions.	13
3–1.	Control Fin Shear Force and Bending Moment.	14
3–2.	General Control Fin Root Characteristics.	15
3–3.	AdKEM Control Fin Root Characteristics.	16
3–4.	Control Fin Bending Stiffness and Deflection Curves.	17
3–5.	Comparison Between Distributed Load and Concentrated Load Cases.	18
4–1.	Block Diagram of Third Order System.	19
4–2.	AdKEM Actuator Schematic.	20
4–3.	AdKEM Small Actuator Dynamic Stiffness for $\delta = .45$.	21
4–4.	AdKEM Small Actuator Dynamic Stiffness for $\delta = .50$.	22
4–5.	AdKEM Small Actuator Dynamic Stiffness for $\delta = .53$.	23
4–6.	AdKEM Small Actuator Dynamic Stiffness for $\delta = 0.0$.	24
4–7.	AdKEM Large Actuator Dynamic Stiffness for $\delta = .20$.	25
4–8.	AdKEM Large Actuator Dynamic Stiffness for $\delta = .25$.	26
4–9.	AdKEM Large Actuator Dynamic Stiffness for $\delta = .29$.	27
4–10.	AdKEM Large Actuator Dynamic Stiffness for $\delta = 0.0$.	28
4–11.	Block Diagram of AdKEM Detailed Non–Linear Actuator Model.	29
5–1.	Fin Flutter Determination Plot.	30

1.0 INTRODUCTION

The purpose of this report is to evaluate the flutter characteristics of a control fin for the Advanced Kinetic Energy Missile (AdKEM). First of all the two–degree–of–freedom equations of motion for a control fin under aerodynamic and actuator loads will be determined. To present a worst case analysis of the problem, these equations will be simplified by neglecting mechanical and aerodynamic damping terms. The fin characteristic equation will then be found and the fin flutter regions will be plotted. Once the flutter regions are plotted, the fin bending stiffness and actuator dynamic stiffness must be known to evaluate the possibility for fin flutter occurring.

The fin bending stiffness is determined assuming a distributed load, equal to the dynamic pressure, is applied to the fin. The fin bending moment equation is integrated numerically to determine the fin slope and resulting bending stiffness at any point along the fin span. These results are then modified for input into the stability equation.

The flutter analysis contained in Appendix A assumes that the actuator's hinge moment stiffness can be represented by a second order system. This report investigates the validity of this assumption by comparing the second order system's stiffness to that of a third order system and a detailed non–linear actuator model. Results indicated that for the case of zero damping, a worst case flutter condition, the second order system model provides a good approximation of the real actuator's dynamic stiffness.

The values found for fin bending stiffness and actuator dynamic stiffness are then compared to the fin stability plot to evaluate the possibility of fin flutter. The results show that the fin design considered in the analysis lies in the flutter region.

2.0 FIN STABILITY EQUATION

The equations of motion of a missile control fin may be determined by considering the fin free–body diagram as shown in Figure 2–1. This figure shows a two–degree–of–freedom control fin with aerodynamic and actuator loads being applied. Appendix A contains two reports entitled Two–Degree–of–Freedom High Speed Flutter Model and ARAP Simplified Criterion which were used as references in the development of the equations of motion. These are

$$\begin{bmatrix} I_{xx} & I_{xy} \\ I_{xy} & I_{yy} \end{bmatrix} \begin{bmatrix} \ddot{\theta} \\ \ddot{\alpha} \end{bmatrix} + \begin{bmatrix} C_\theta + (Q/V_m \ A \ CL_\alpha)\beta_{yy} & (Q/V_m \ A \ CL_\alpha)\beta_{xy} \\ (Q/V_m \ A \ CL_\alpha)\beta_{xy} & C_\alpha + (Q/V_m \ A \ CL_\alpha)\beta_{xx} \end{bmatrix} \begin{bmatrix} \dot{\theta} \\ \dot{\alpha} \end{bmatrix}$$

$$+ \begin{bmatrix} K_\theta & Q \ A \ CL_\alpha \ Y_{ac} \\ 0 & K_d + Q \ A \ CL_\alpha \ X_{ac} \end{bmatrix} \begin{bmatrix} \theta \\ \alpha \end{bmatrix} = 0 \qquad (2-1)$$

These equations can be simplified by assuming that all damping terms are zero. This results in the equations

$$\begin{bmatrix} I_{xx} & I_{xy} \\ I_{xy} & I_{yy} \end{bmatrix} \begin{bmatrix} \ddot{\theta} \\ \ddot{\alpha} \end{bmatrix} + \begin{bmatrix} K_\theta & Q \ A \ CL_\alpha \ Y_{ac} \\ 0 & K_d + Q \ A \ CL_\alpha \ X_{ac} \end{bmatrix} \begin{bmatrix} \theta \\ \alpha \end{bmatrix} = 0 \qquad (2-2)$$

The fin characteristic equation can now be determined and written in Laplace form as

$$(I_{xx}I_{yy} - I_{xy}{}^2)s^4 + (I_{xx}K_{\alpha\alpha} + I_{yy}K_\theta - I_{xy}K_{\alpha\theta})s^2 + K_{\alpha\alpha}K_\theta = 0 \qquad (2-3)$$

where

$$K_{\alpha\alpha} = K_d + Q \ A \ CL_\alpha \ X_{ac} \qquad (2-4)$$

$$K_{\alpha\theta} = Q \ A \ CL_\alpha \ Y_{ac} \qquad (2-5)$$

The dynamic pressure, Q, is a function of the Mach number and is found using

$$Q = \tfrac{1}{2} n_{air} \ P_{atm} \ Mach^2 \qquad (2-6)$$

The lift coefficient, CL_α, center of pressure, and fin surface area and inertias of the fin shown in Figure 2–2 have been estimated as shown in Table 2–1

TABLE 2-1. Control Fin Characteristics

MACH NUMBER	$CL\alpha(rad^{-1})$	X_{ac} (in)
0.5	4.0508	-0.60
1.0	4.9217	-0.78
1.5	4.5321	0.15
2.0	3.3232	0.28
3.0	2.1257	0.26
4.0	1.5699	0.204
5.0	1.2433	0.17
6.0	1.0428	0.15
6.5	0.9740	0.145
7.0	0.8995	0.14

Fin Reference Area = 3.463 in^2
Y_{ac} = 0.9 in
I_{xx} = 285.43 (10^{-6}) in–lb_f–s^2
I_{yy} = 122.77 (10^{-6}) in–lb_f–s^2
I_{xy} = 28.672 (10^{-6}) in–lb_f–s^2

The location of the center of pressure in the x–axis, X_{ac}, is measured from the fin hinge line and is positive to the rear as shown in Figure 2–1. The roots of Equation 2–3 can now be solved for as a function of fin bending stiffness, actuator stiffness, and Mach number and the stability regions of the control fin can be plotted. A listing of the program used to determine the roots of Equation 2–3 is provided in Appendix B and the results are plotted in Figure 2–3.

3.0 CONTROL FIN BENDING STIFFNESS

The fin bending stiffness, K_θ, must be found in order to determine if the control fin design is unstable. Bending stiffness is defined as

$$K_\theta(y) = [dM/d\theta]\,|_y \tag{3-1}$$

The distance y is measured across the fin span from the root as indicated in Figure 2–1. The equation for the bending moment, assuming a constant distributed load, Q, applied to the fin, may be found by integrating the shear equation for the steel control fin root shown in Figure 3–1. In order to evaluate the shear, the fin planar area must be determined. This is

$$A(y) = \tfrac{1}{2}\, y\,[2l_r + (l_t - l_r)\, y/l_S] \tag{3-2}$$

Now the shear equation can be found by considering the force balance at a point y along the span.

$$V(y) = Q\,[A(l_S) - A(y)] \tag{3-3}$$

where $A(l_s)$ is the total fin root area. Integration of Equation 3–3 results in the bending moment equation as a function of y.

$$M(y) = Q\,[A(l_S)\,(y - l_S) - \tfrac{1}{2}\, l_r\,(y^2 - l_S^2) - (l_t - l_r)\,(y^3 - l_S^3)/6l_S] \tag{3-4}$$

Next, the fin slope must be determined. The difference in slope of two points along the fin root is defined as

$$\theta_b - \theta_a = \int_{Y_a}^{Y_b} (M/EI)\, dy \tag{3-5}$$

At the fin root the slope, θ_a, is assumed zero. Therefore, the slope at any location y may be calculated as

$$\theta(y) = (1/E) \int_0^Y (M/I)\,dy \tag{3-6}$$

assuming that the modulus of elasticity, E, is constant. Since both the bending moment and the moment of inertia are functions of y, Equation 3–6 could be better solved using numerical integration. In that case, Equation 3–6 takes the form

$$\theta(y) = (\delta y/E) \sum_{j=0}^{Y} [M/I]_j \tag{3–7}$$

where δy is the integration step size. In order to determine the slope at a point on the fin, the cross–sectional moment of inertia must be found as it varies with span. The development of these equations for the fin root in Figure 3–2 is shown in Appendix C.

Knowing the bending moment and slope at any location, the bending stiffness may be calculated from Equation 3–1. This equation can also be expressed as

$$K_\theta(y) = [M(y) - M(y-\delta y)]/[\theta(y) - \theta(y-\delta y)] \tag{3–8}$$

where the notation '$(y-\delta y)$' denotes the moment or slope at the previous integration point. Note that the dynamic pressure, Q, cancels out in the calculation of bending stiffness.

The equations discussed above have been incorporated into a computer program, listed in Appendix D, which calculates the fin bending stiffness and other parameters. This program first calculates the cross–sectional moment of inertia at the particular span location using the equations developed in Appendix C. Then the bending moment at that location is calculated from Equation 3–4. This is used in Equation 3–7 to calculate the slope of the point and the bending stiffness is determined using Equation 3–8. Also calculated is the deflection of the fin normalized to dynamic pressure. These data are then written to a file for plotting. This process is repeated along the length of the span.

The fin geometry parameters shown in Figure 3–3 were used as input to the program discussed above and the results are shown in Figure 3–4. This plot shows the fin bending stiffness and normalized deflection as they vary along the span.

Since the fin characteristic equation developed in Section 1.0 assumes that the dynamic pressure is resolved as the lift force applied at the center of pressure, a comparison of the two methods has to be made. This can be done by letting the deflection of the distributed load case at the fin tip equal the deflection of the simple case at the fin tip and solving for the bending stiffness that would allow this deflection to occur. This is shown pictorially in Figure 3–5. Summing moments about the fin root for the simple case shows that

$$F_L \, Y_{ac} = K_{\theta S} \, \theta_S \tag{3–9}$$

Solving for the spring stiffness, $K_{\theta S}$, by relating the lift force to dynamic pressure and the bending angle to deflection shows that

$$K_{\theta S} = [A(l_S) \, Y_{ac} \, l_S]/[z(l_S)/Q] \tag{3–10}$$

where $z(l_S)/Q$ is the absolute value of the normalized deflection of the fin at the tip and is taken from Figure 3–4. Taking the value of $z(l_S)/Q$ from this figure shows

$$z(l_S)/Q = -0.910(10^{-3})$$

and substituting this into Equation 3–10 results in an equivalent spring stiffness of

$$\boxed{K_{\theta S} = 5280 \text{ in–lb}_f/\text{rad}}$$

This value can now be used in conjunction with the actuator dynamic stiffness to determine, using Figure 2–3, if the fin design lies in the flutter regions.

4.0 ACTUATOR DYNAMIC STIFFNESS

The flutter analysis contained in Appendix A uses a second order linear system to represent the actuator's hinge moment stiffness. The intent of this section is to determine how well a second order system represents the dynamic stiffness of an actual open center valve pneumatic actuator. To accomplish this the second order system's dynamic stiffness is determined and compared to that of a linearized actuator model, as well as a detailed non–linear actuator model.

The second order system's dynamic stiffness is determined by considering the equation of motion of a second order system subjected to a torque disturbance.

$$I_{yy}\ddot{\alpha} + C_\alpha\dot{\alpha} + K_\alpha\alpha = T_0\cos(\Omega t) \qquad (4\text{–}1)$$

The steady–state solution to this equation is given by

$$\alpha_{ss} = \alpha_a \cos(\Omega t - \phi) \qquad (4\text{–}2)$$

Substituting Equation 4–2 and its derivatives into Equation 4–1 results in

$$-I_{yy}\Omega^2\alpha_a \cos(\Omega t - \phi) - C_\alpha\Omega\alpha_a \sin(\Omega t - \phi) + K_\alpha\alpha_a \cos(\Omega t - \phi) = T_0\cos(\Omega t) \quad (4\text{–}3)$$

Since each term in this equation represents a force acting on the inertia, the equation can be represented by a force vector polygon, from which it is easily seen that

$$T_0^2 = (K_\alpha\alpha_a - I_{yy}\Omega^2\alpha_a)^2 + (C_\alpha\Omega\alpha_a)^2 \qquad (4\text{–}4)$$

and

$$\tan(\phi) = C_\alpha\Omega/(K_\alpha - I_{yy}\Omega^2) \qquad (4\text{–}5)$$

Solving for the amplitude of the steady–state fin position, α_a, and recalling expressions for frequency ratio, natural frequency and damping factor results in

$$\alpha_a = (T_0/K_\alpha)/[(1-r^2)^2 + (2\delta r)^2]^{\frac{1}{2}} \qquad (4\text{–}6)$$

From Equation 4–6 the desired expression for the second order system's dynamic stiffness is obtained

$$K_d = (T_0/\alpha_a) = K_\alpha\,[(1-r^2)^2 + (2\delta r)^2]^{1/2} \qquad (4\text{–}8)$$

An expression for the dynamic stiffness of the third order, linearized actuator model, represented by the block diagram in Figure 4–1, was obtained from Reference 1 and is given by

$$K_d = (1/s)\,(I_{yy}s^3 + Bs^2 + (K_\alpha - H_\alpha)\ s + K_\alpha K_a G_c) \qquad (4\text{–}9)$$

Setting s equal to $j\Omega$, an expression for the magnitude of Equation 4–9 is obtained, which is the desired expression for the third order system's dynamic stiffness.

$$K_d = \left\{(K_\alpha + H_\alpha - I_{yy}\,\Omega^2)^2 + [B\Omega - (K_\alpha K_a G_c/\Omega)]^2\right\}^{\frac{1}{2}} \qquad (4\text{–}10)$$

Substituting expressions for frequency ratio, natural frequency and damping factor, which were defined for the second order system, Equation 4–10 becomes

$$K_d = K_\alpha\left\{[1 - r^2 + (H_\alpha/K_\alpha)]^2 + [2\delta r - (K_a G_c/\Omega)]\right\}^{\frac{1}{2}} \qquad (4\text{–}11)$$

Note that for the condition where H_α is small compared to K_α, the dynamic stiffness determined by Equation 4–11 approaches that of Equation 4–8 at high frequencies. However, at low frequencies the dynamic stiffness determined by Equation 4–11 approaches infinity, while Equation 4–8 approaches K_α.

In order to apply Equations 4–8 and 4–11, an expression for the actuator's static stiff–ness must be determined. From the diagram shown in Figure 4–2, an expression for torque about the hinge line is determined.

$$T = [A_cP_c - (A_c - A_r)P_S]\,L \qquad (4\text{–}12)$$

Differentiating this equation with respect to α results in

$$dT/d\alpha = A_c L(dP_c/d\alpha) \tag{4-13}$$

From the actuator geometry, a differential change in volume is related to a differential change in actuator position according to the relation

$$d\alpha/dV = -1/A_c L\sec^2(\alpha) \tag{4-14}$$

If the compression of the gas above the piston follows an isentropic process then pressure and volume are related according to

$$P_c V^n = \text{constant} \tag{4-15}$$

Differentiation of Equation 4–15 results in

$$dP_c/dV = -nP_c/V \tag{4-16}$$

Combining Equations 4–13, 4–14, and 4–16 provides an expression for the actuator's static stiffness.

$$K_\alpha = nP_c(LA_c)^2\sec^2(\alpha)/V \tag{4-17}$$

The dynamic stiffness was determined for the small and large AdKEM pneumatic actuators using Equations 4–8, 4–11, and 4–17. The following parameters were used for the small actuator.

P_c = 1587.3 psia	L = 0.6 in	A_c = 0.2961 in^2
V_o = 0.046 in^3	n = 1.667	B = 0.50 in–lb$_f$/rad/s
H_α = 0 in–lb$_f$/rad	G_c = 1.0	K_a = 124.64 rad^2/s
I_{yy} = $122.77(10)^{-6}$ in–lb$_f$–s^2		

From which the small actuator's static stiffness and natural frequency are determined at the null position ($\alpha = 0°$).

$$\boxed{\begin{array}{c} K_\alpha = 1808 \text{ in–lb}_f/\text{rad} \\ \Omega_n = 611 \text{ Hz} \end{array}}$$

The small actuator's dynamic stiffness obtained from the second order model is compared to that of the third order model in Figures 4–3 thru 4–5 for various values of δ. A good match is seen for $\delta = 0.50$, which requires that $C_\alpha = 0.47$. A comparison for the case of zero damping is shown in Figure 4–6.

The large actuator's dynamic stiffness was determined based on the following parameters.

$P_c = 1492.2$ psia	$L = 0.560$ in	$A_c = 0.586$ in^2
$V_o = 0.085$ in^3	$n = 1.667$	$B = 0.50$ in–lb$_f$/rad/s
$H_\alpha = 0$ in–lb$_f$/rad	$G_c = 1.0$	$K_a = 124.64$ rad^2/s
$I_{yy} = 245.54(10)^{-6}$ in–lb$_f$–s^2		

From which the large actuator's static stiffness and natural frequency are determined at the null position ($\alpha = 0^\circ$).

$$\boxed{\begin{array}{c} K_\alpha = 3138 \text{ in–lb}_f\text{/rad} \\ \Omega_n = 569 \text{ Hz} \end{array}}$$

The large actuator's dynamic stiffness obtained from the second order model is compared to that of the third order model in Figures 4–7 thru 4–9 for various values of δ. A good match is seen for δ = 0.25, which requires that $C_\alpha = 0.44$. A comparison for the case of zero damping is shown in Figure 4–10.

As a final comparison the stiffness of the small AdKEM actuator was determined using a detailed non–linear actuator model. A block diagram of this model is shown in Figure 4–11. The stiffness was determined by applying a torque disturbance and determining the resulting deflection. Simulation results are shown compared to the second and third order models in Figures 4– 4 and 4–6 for δ = 0.50 and δ = 0 respectively. Note that for the case with damping the detailed non–linear model indicates a sharp drop in stiffness at the closed loop system's natural frequency, which is not predicted by the linear models. However, for the case of zero damping the models are in fairly close agreement.

Based on the above discussion it may be concluded that the linear second order system model used in the flutter analysis realistically represents the stiffness of the AdKEM actuator for the case of zero damping. Further, since zero damping is a worst case for flutter, the use of a second order system model with zero damping should provide a conservative flutter prediction.

5.0 CONCLUSIONS AND RECOMMENDATIONS

Referring to the values of control fin bending stiffness and actuator dynamic stiffness determined and comparing them to the fin stability regions shows that the fin lies in the flutter region for the small actuator design. This is shown in Figure 5-1 It is also seen that the large actuator design is very close to the flutter regions. One way of eliminating this problem is to increase or decrease the actuator stiffness. Since actuator stiffness is largely a function of the hinge moment requirement this value can not be readily changed. Therefore, it is required that the fin bending stiffness be changed. Referring to Figure 5-1 shows that the best approach would be to increase the fin bending stiffness because this would avoid the flutter regions should the hinge moment requirement, and thus the actuator stiffness, be reduced. Therefore, it is recommended that the fin root thickness be increased and the flutter analysis be performed again.

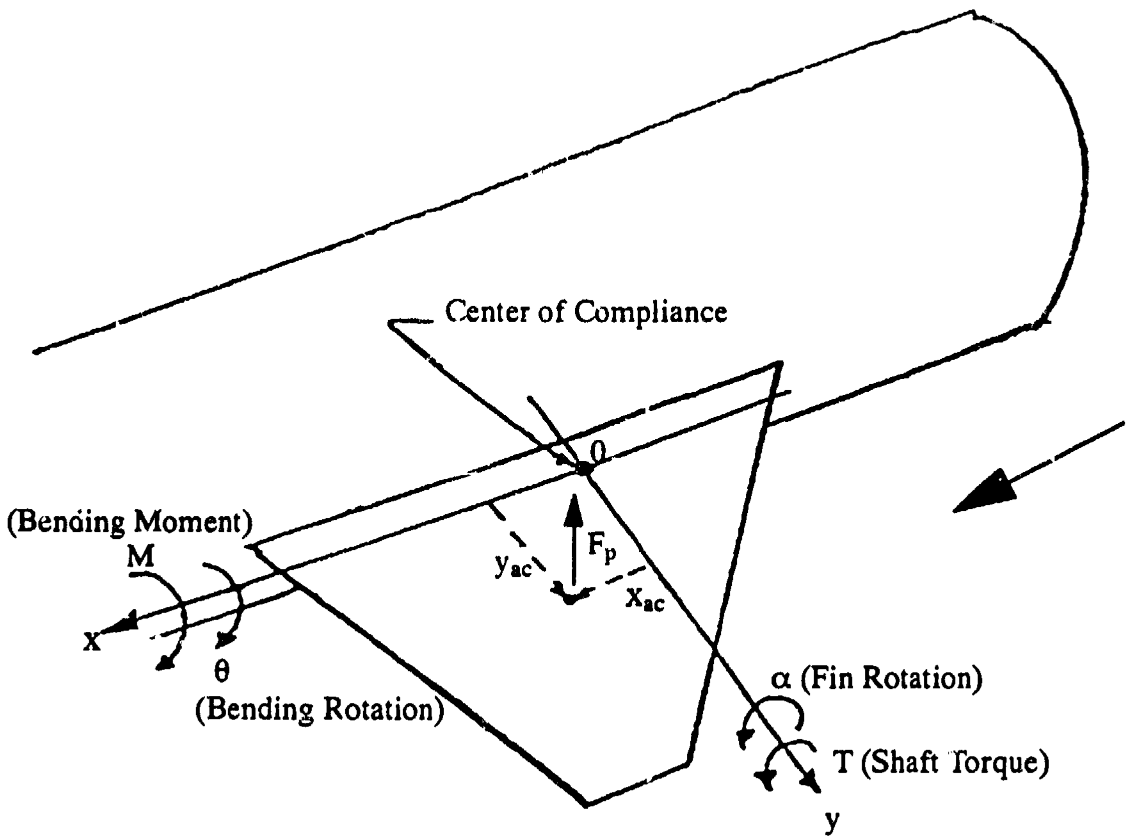

Figure 2–1. Two–Degree–of–Freedom Control Fin.

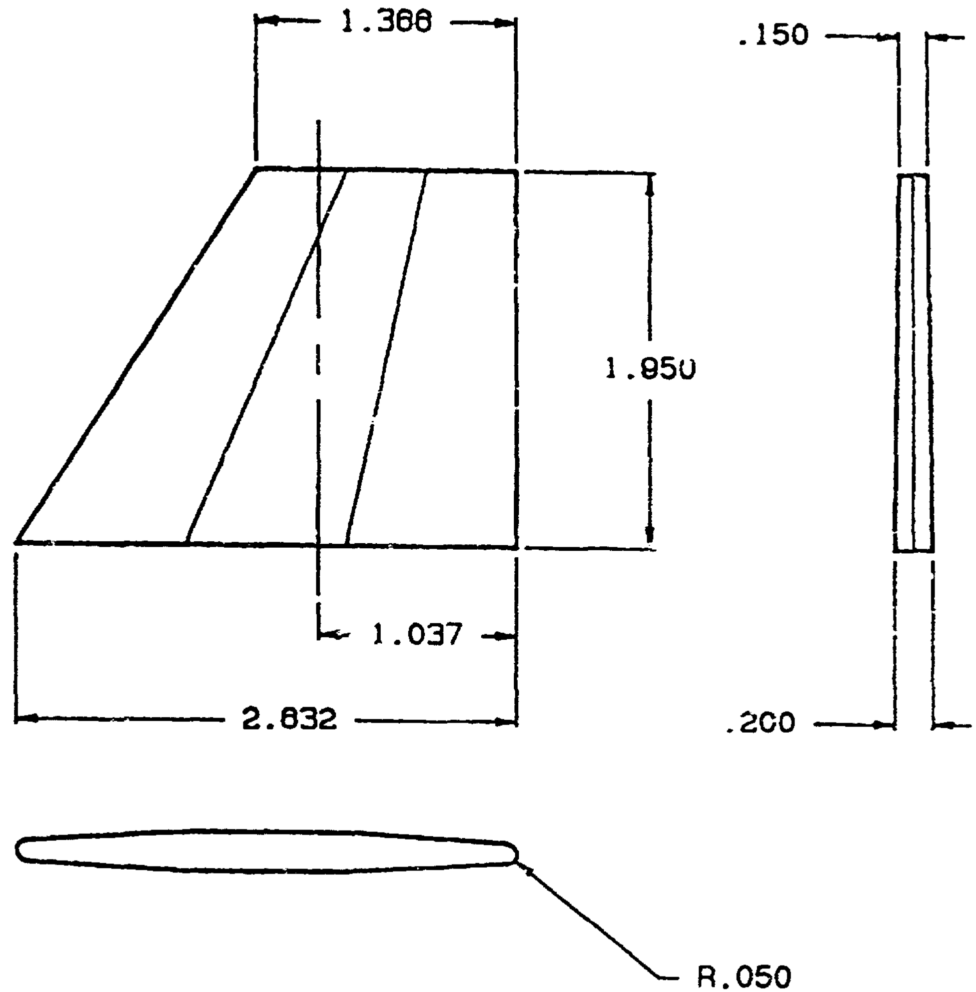

Figure 2–2. AdKEM Control Fin.

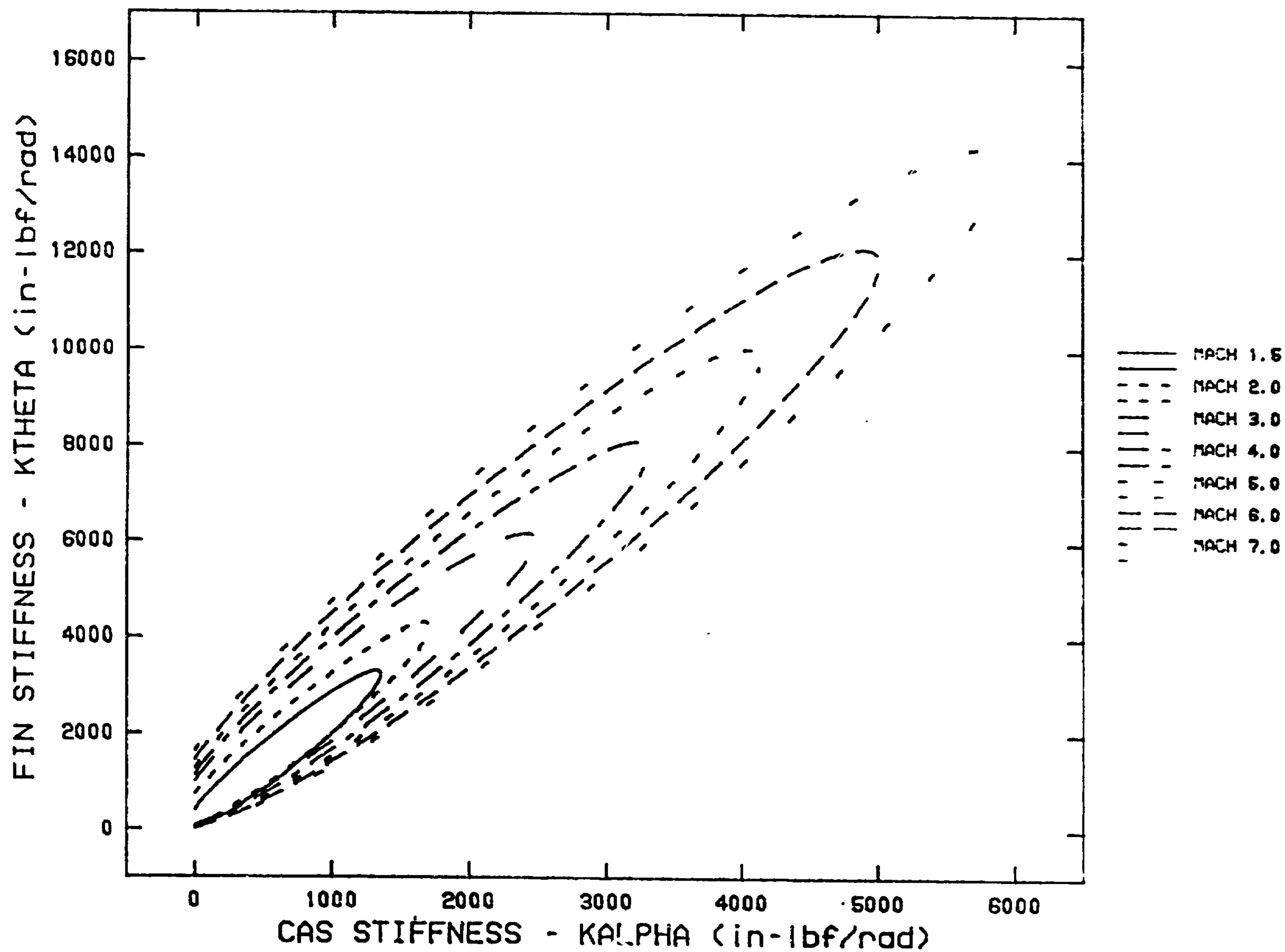

Figure 2–3. AdKEM Control Fin Stability Regions.

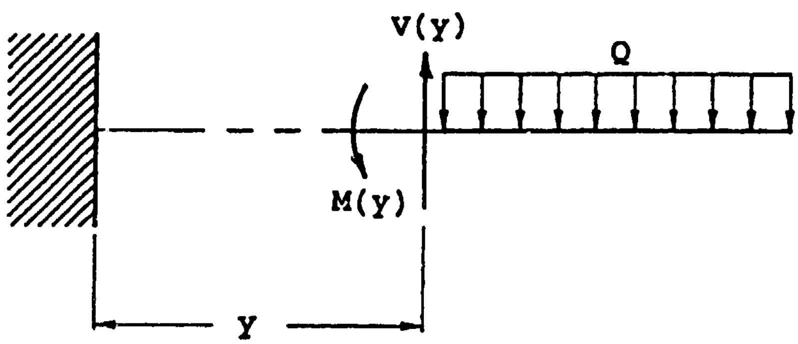

Figure 3–1. Control Fin Shear Force and Bending Moment.

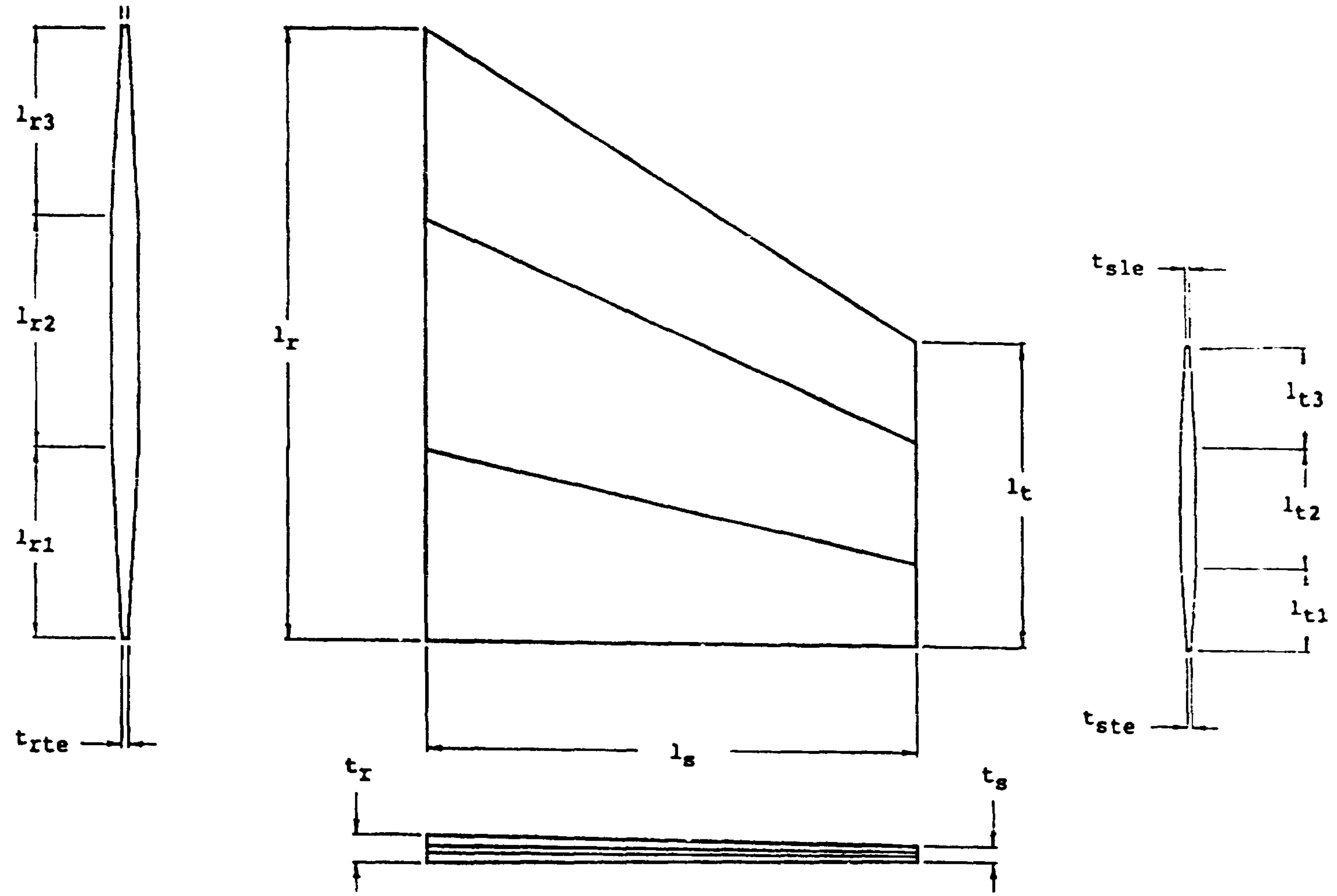

Figure 3–2. General Control Fin Root Characteristics.

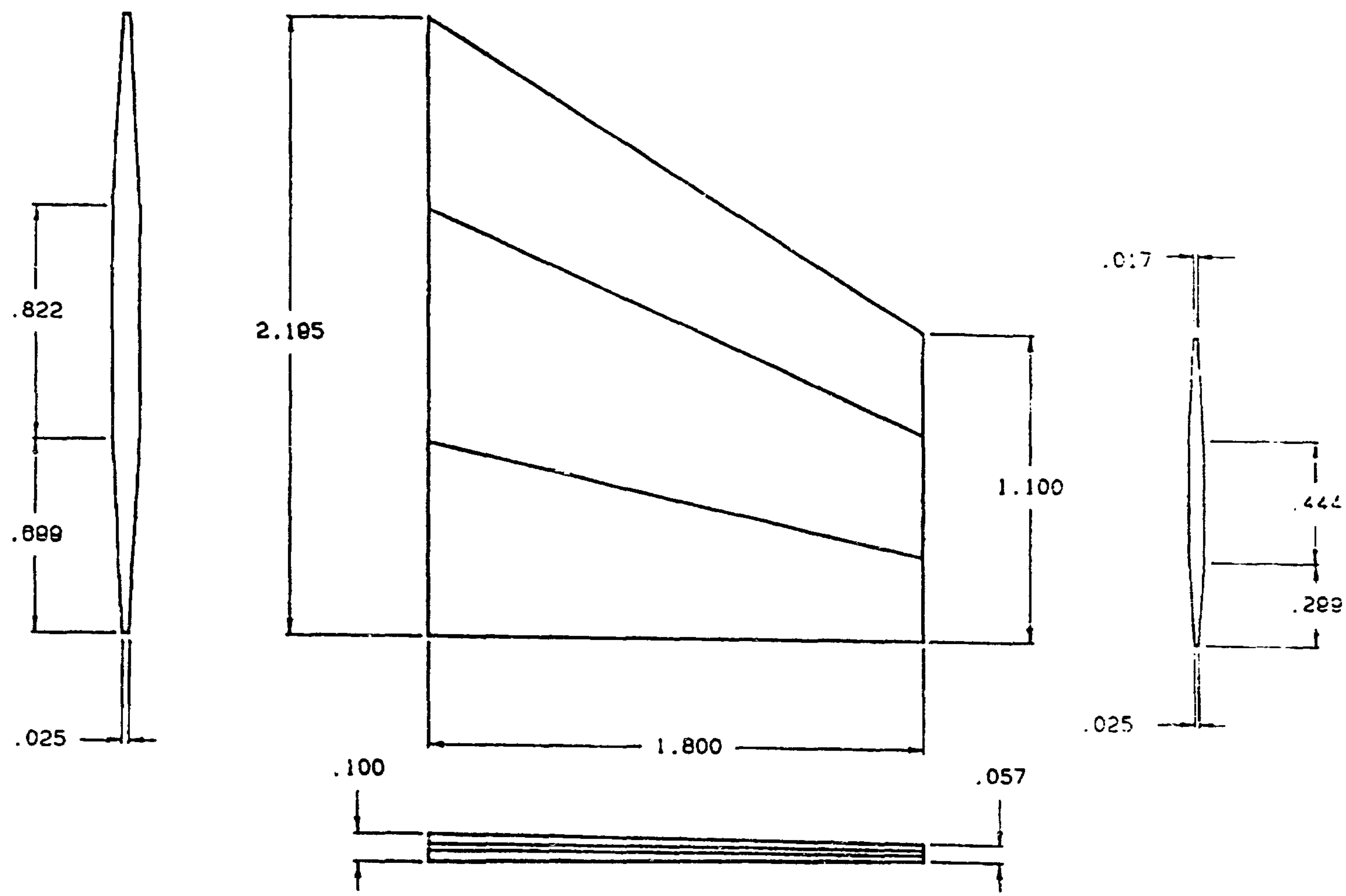

Figure 3–3. AdKEM Control Fin Root Characteristics.

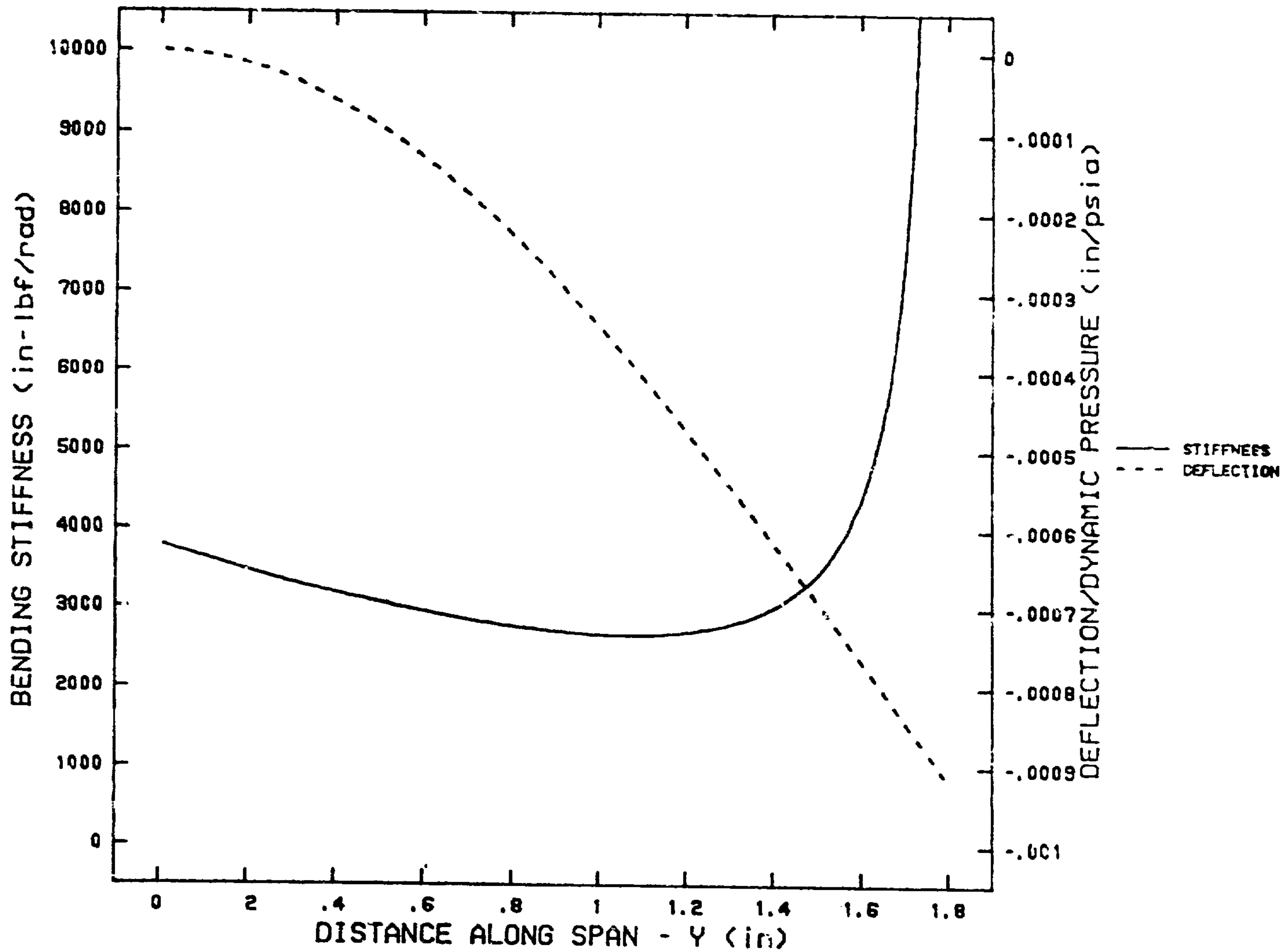

Figure 3–4. Control Fin Bending Stiffness and Deflection Curves.

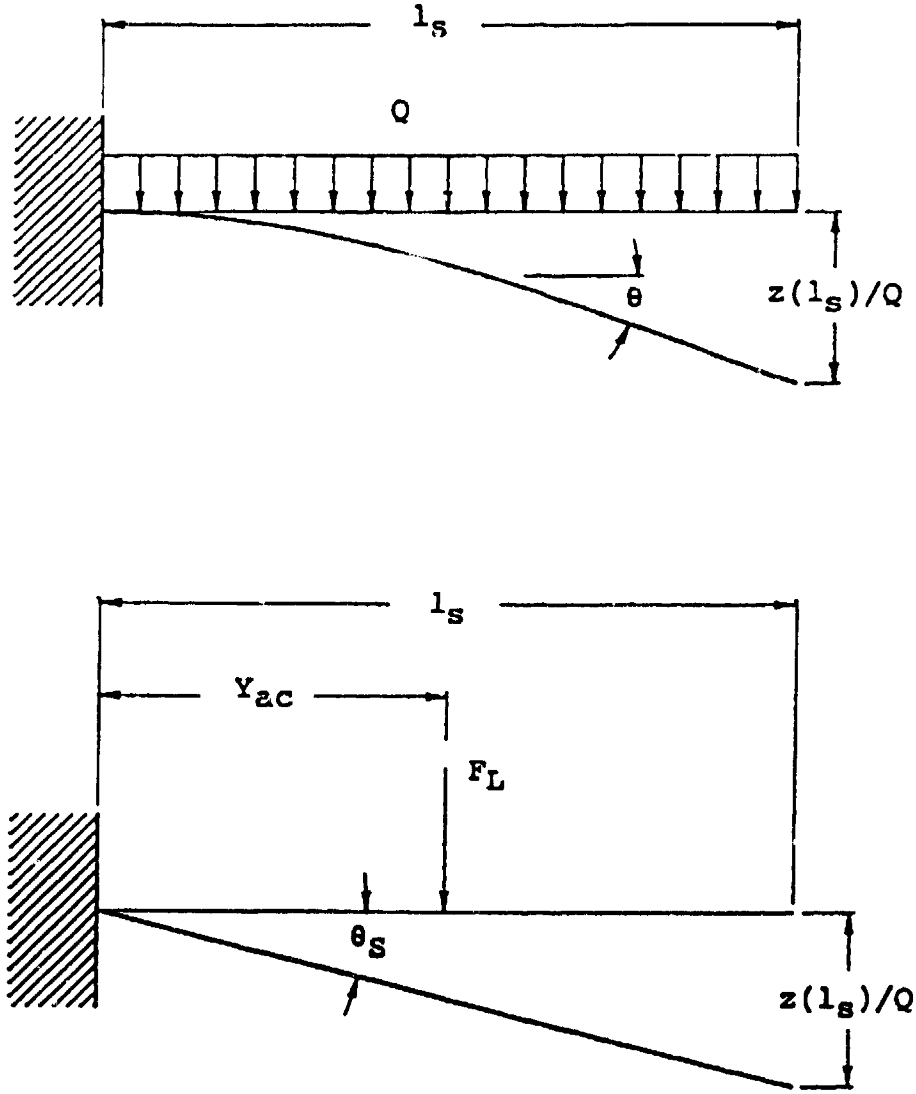

Figure 3–5. Comparison Between Distributed Load and Concentrated Load Cases.

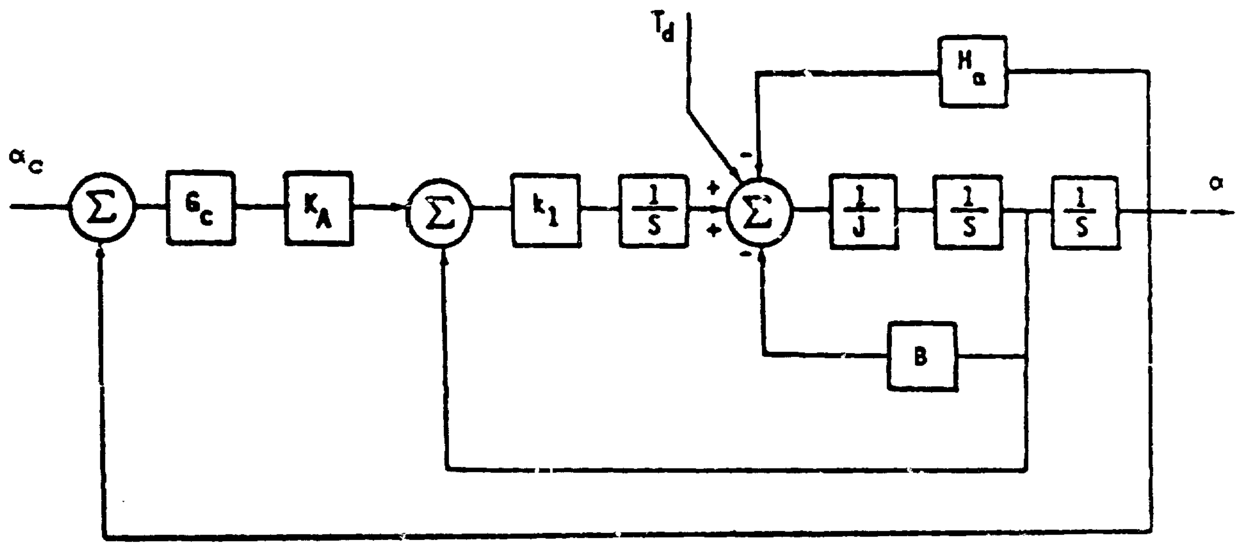

Figure 4–1. Block Diagram of Third Order System.

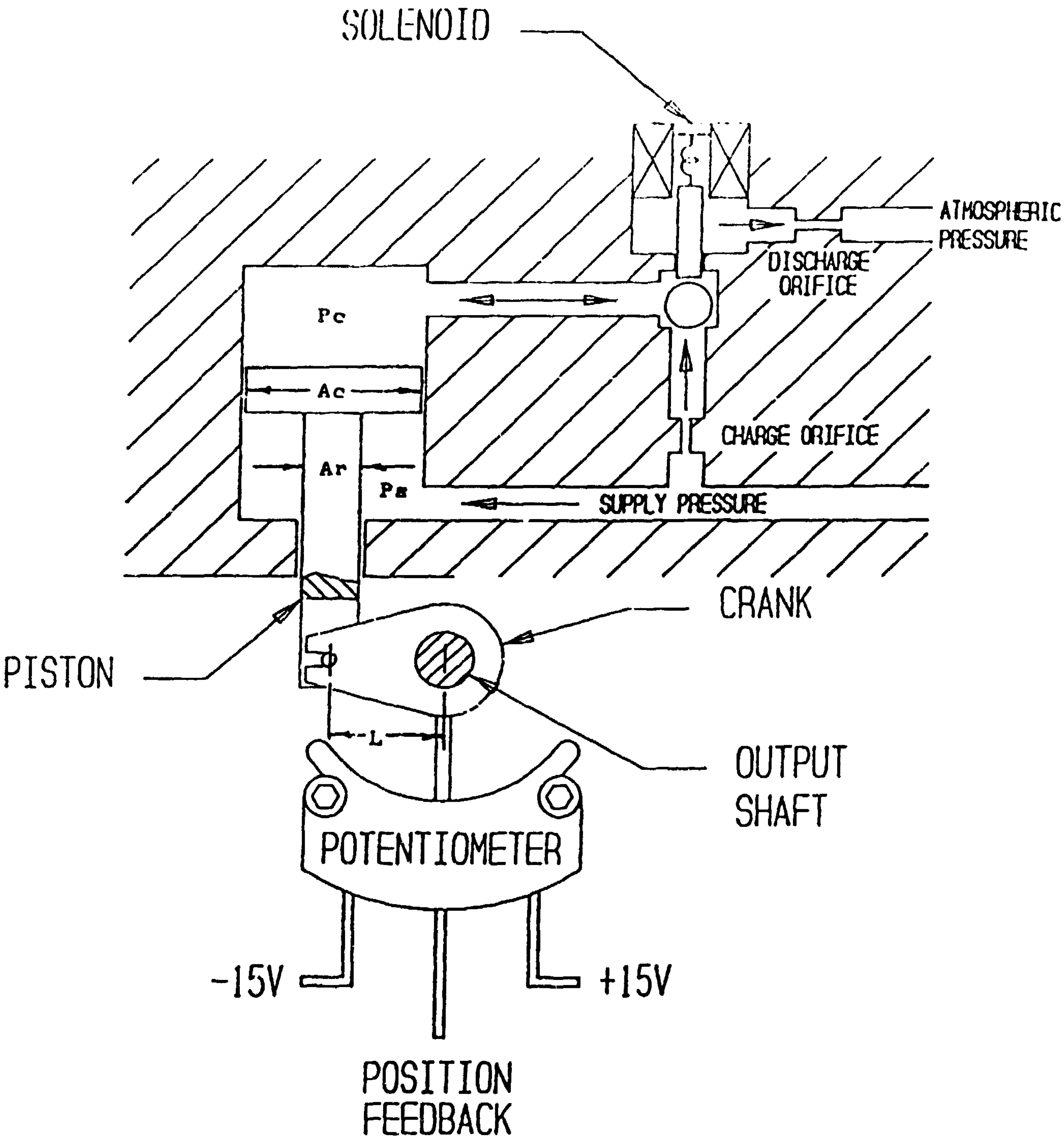

Figure 4–2. AdKEM Actuator Schematic.

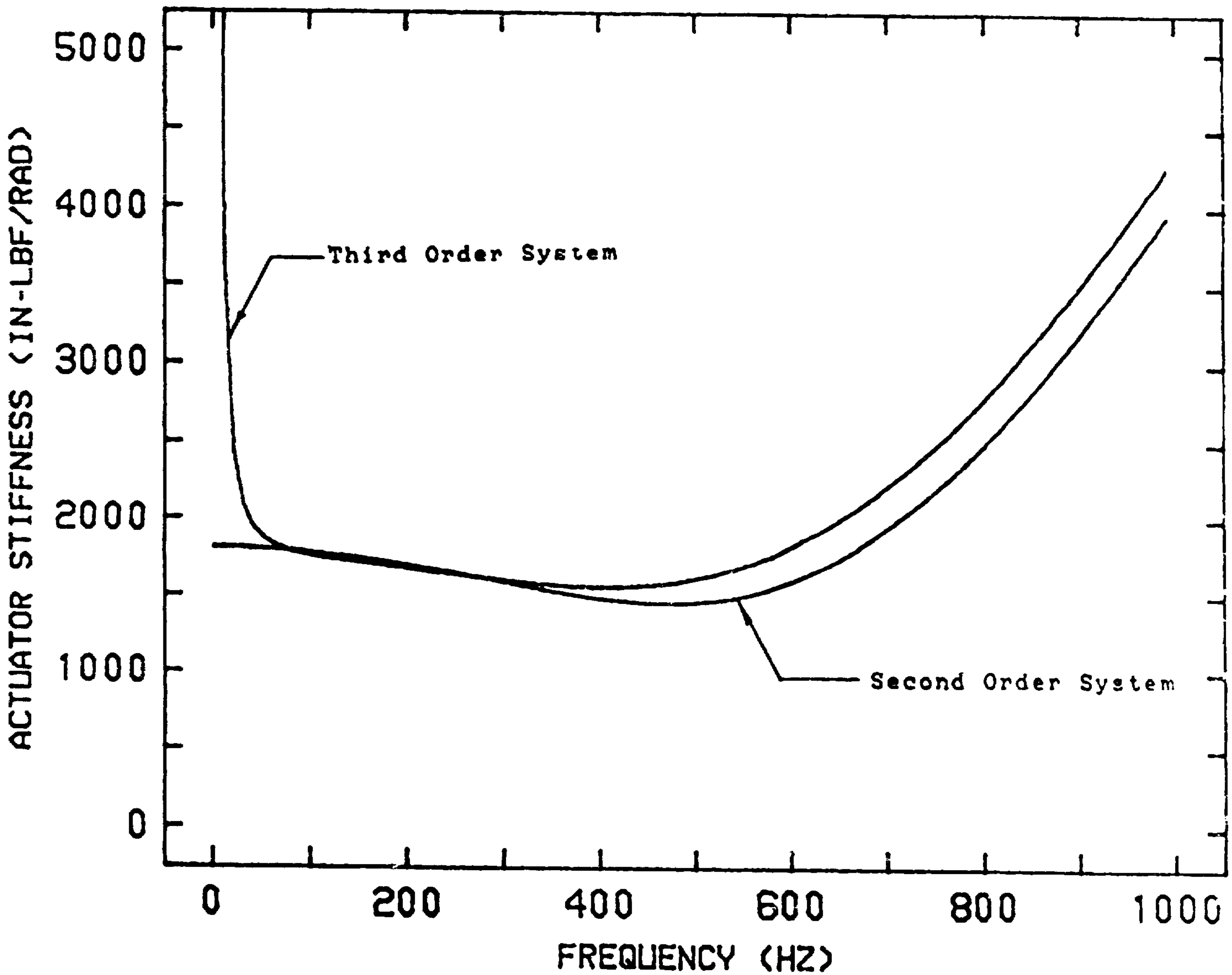

Figure 4–3. AdKEM Small Actuator Dynamic Stiffness for $\delta = .45$.

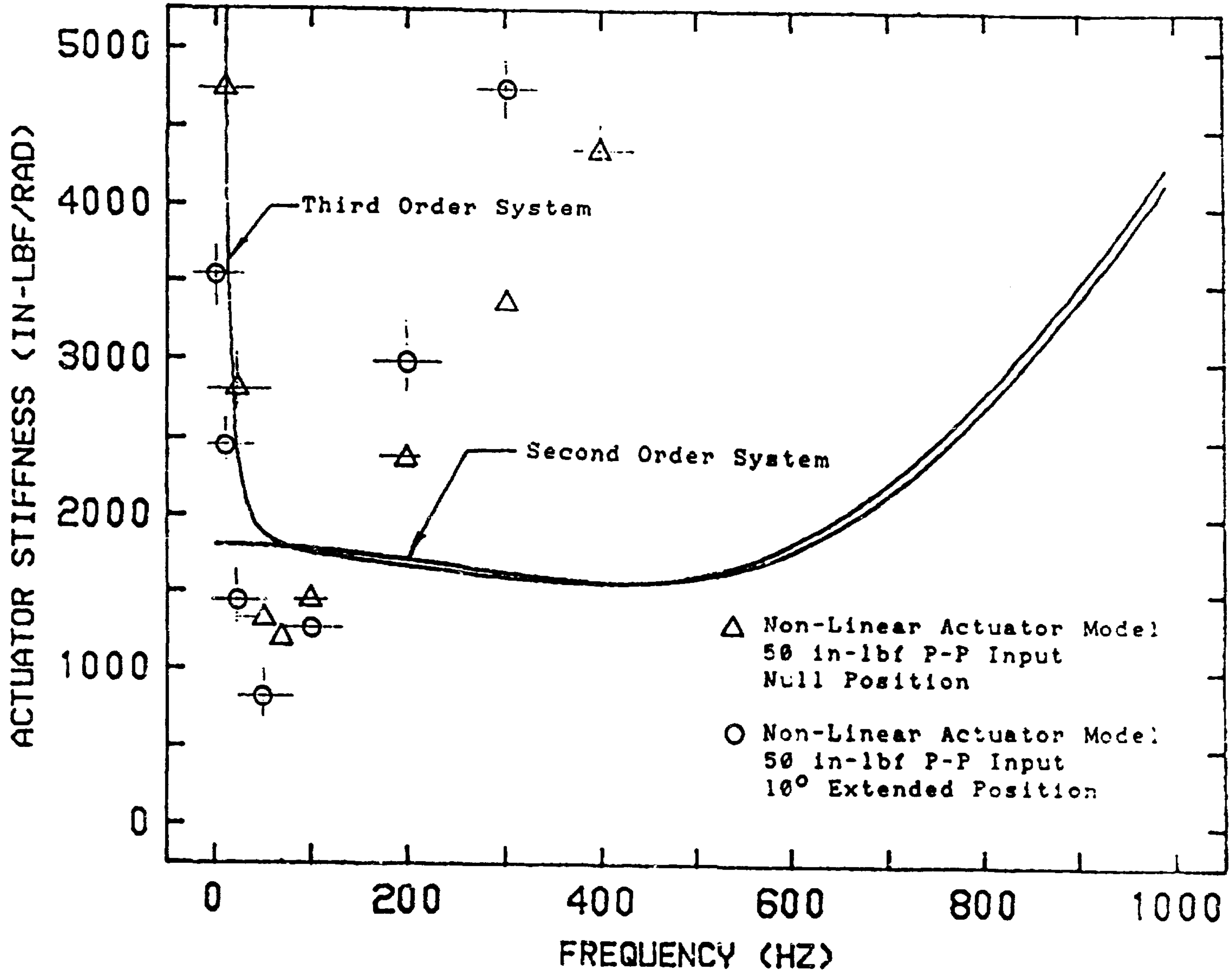

Figure 4–4. AdKEM Small Actuator Dynamic Stiffness for δ = .50.

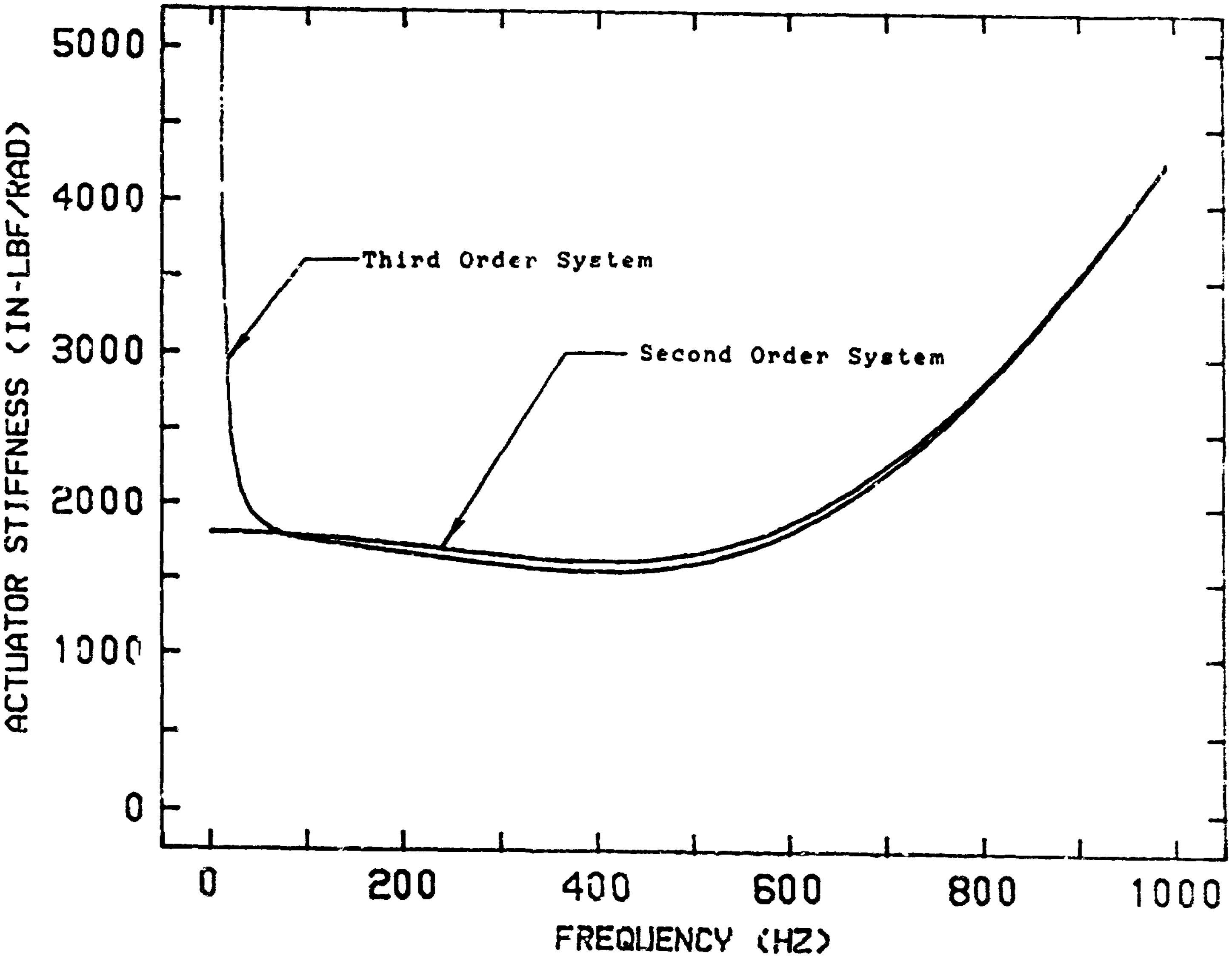

Figure 4–5. AdKEM Small Actuator Dynamic Stiffness for $\delta = .53$.

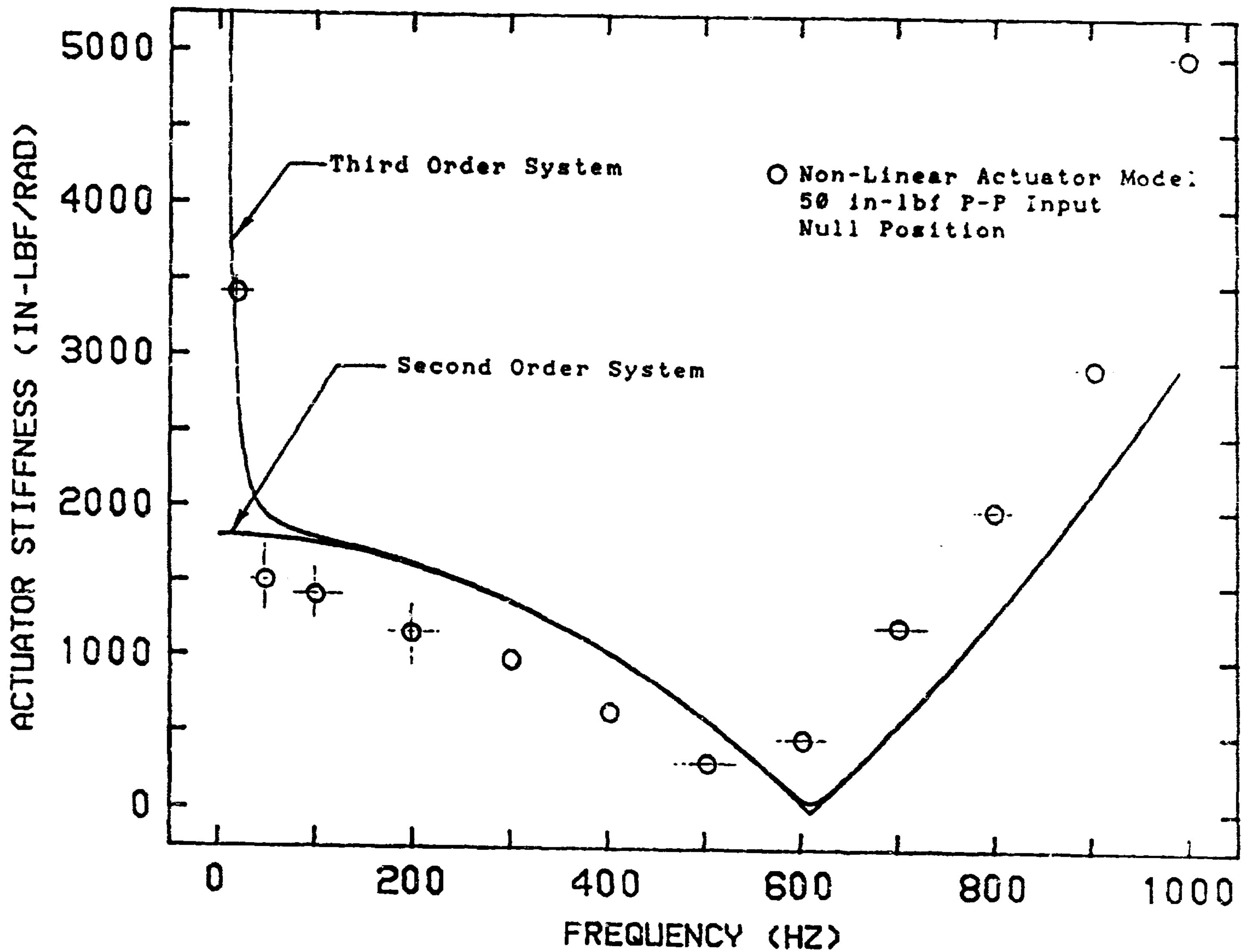

Figure 4–6. AdKEM Small Actuator Dynamic Stiffness for $\delta = 0.0$.

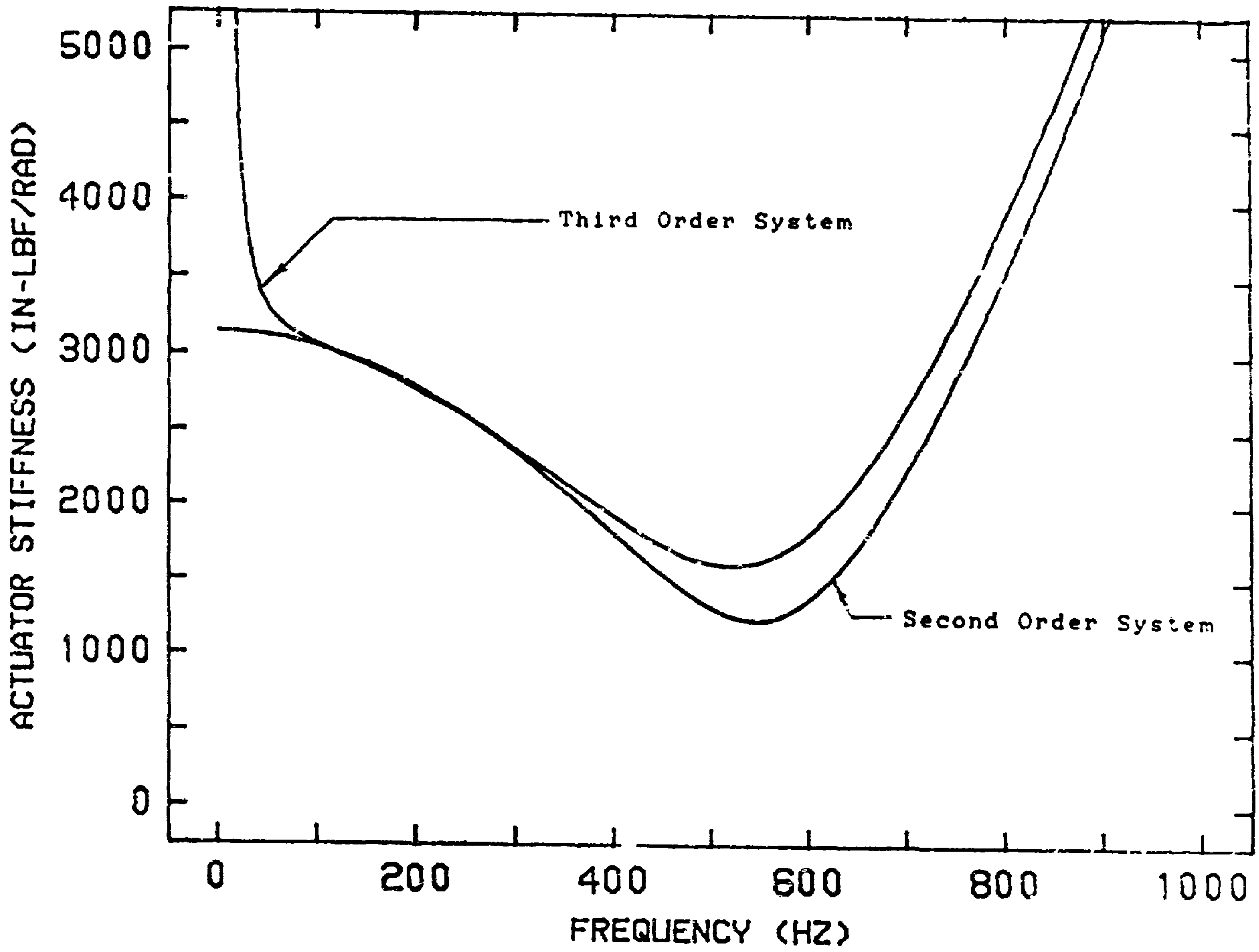

Figure 4–7. AdKEM Large Actuator Dynamic Stiffness for $\delta = .20$.

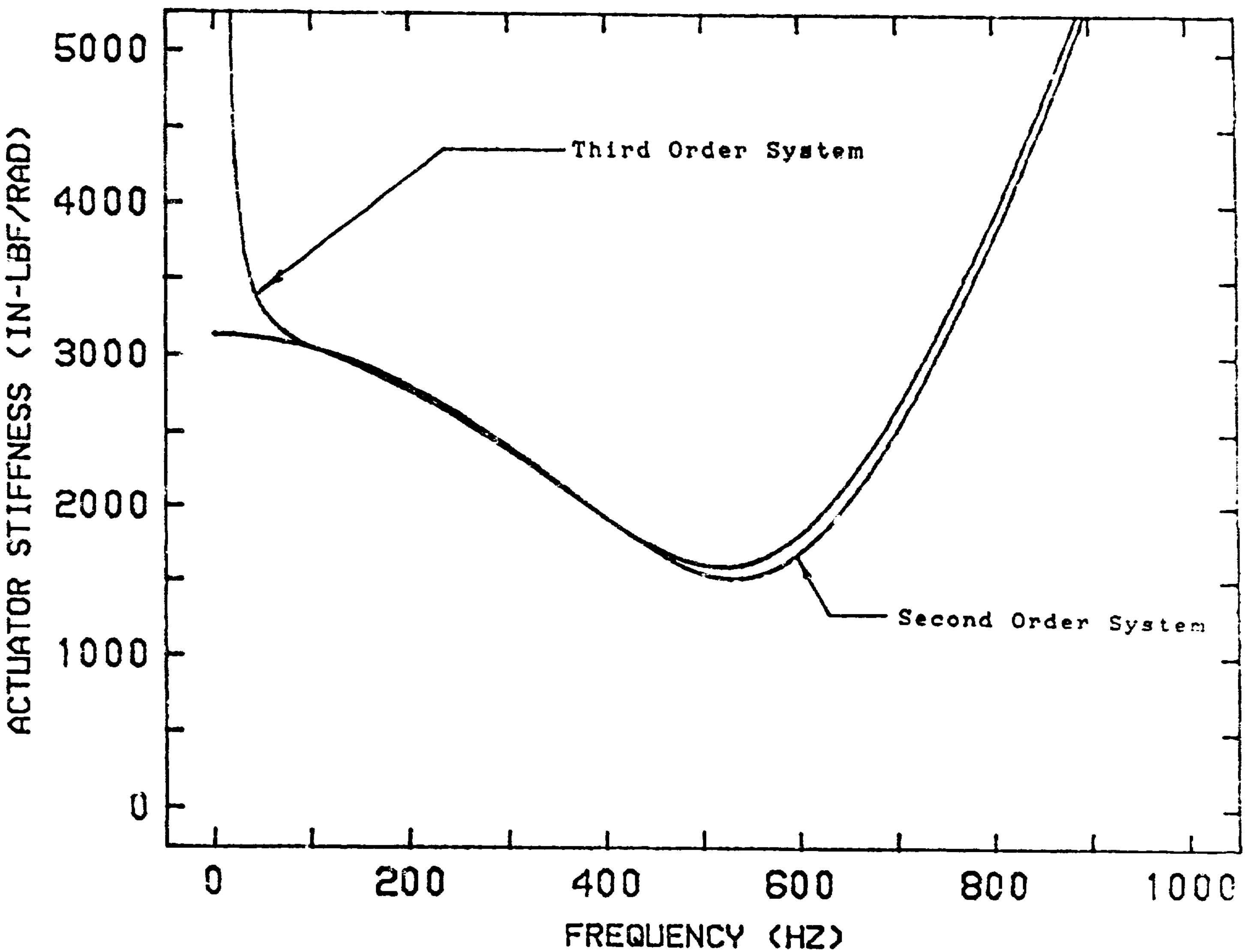

Figure 4–3. AdKEM Large Actuator Dynamic Stiffness for δ = .25.

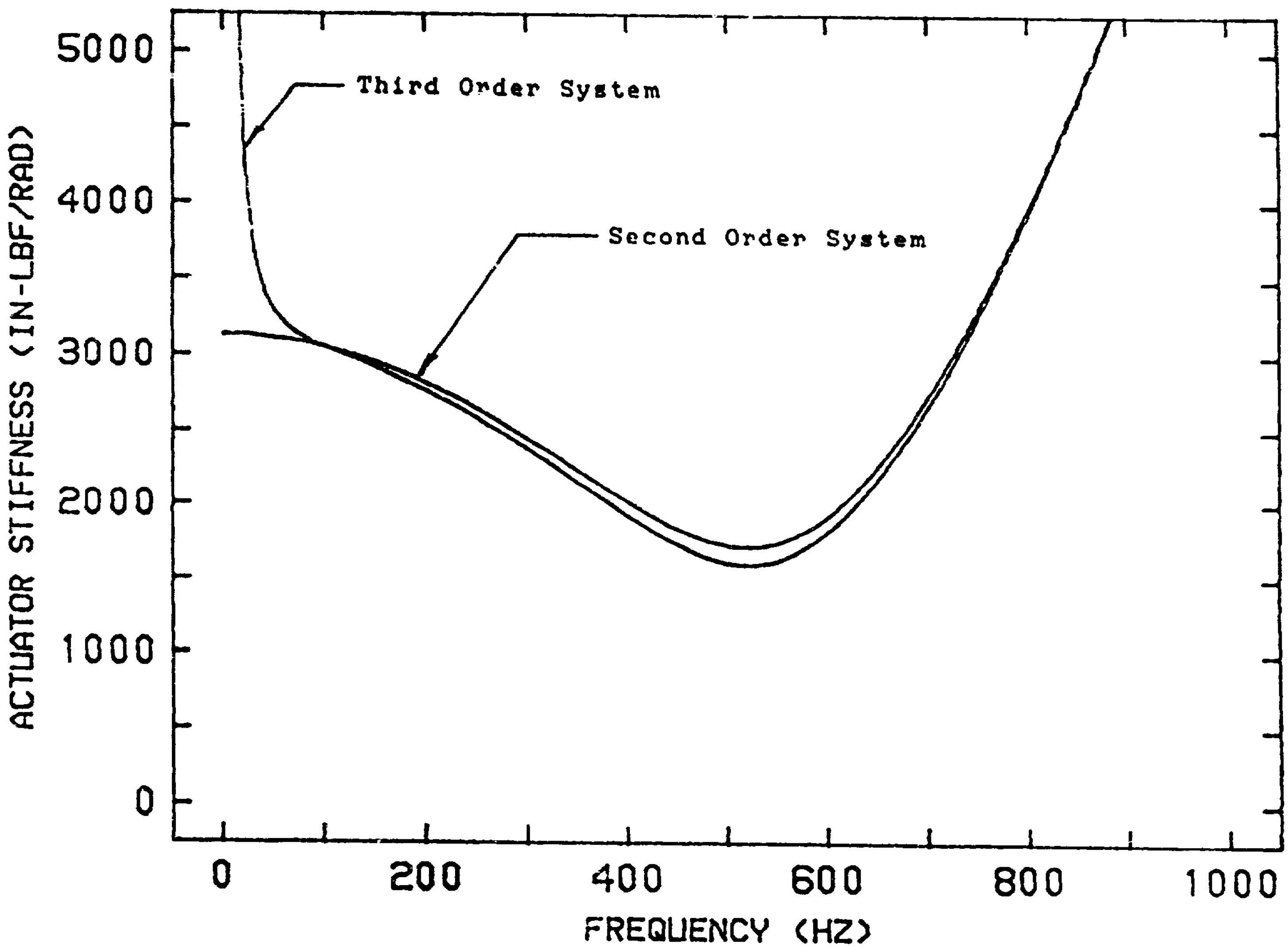

Figure 4–9. AdKEM Large Actuator Dynamic Stiffness for δ = .29.

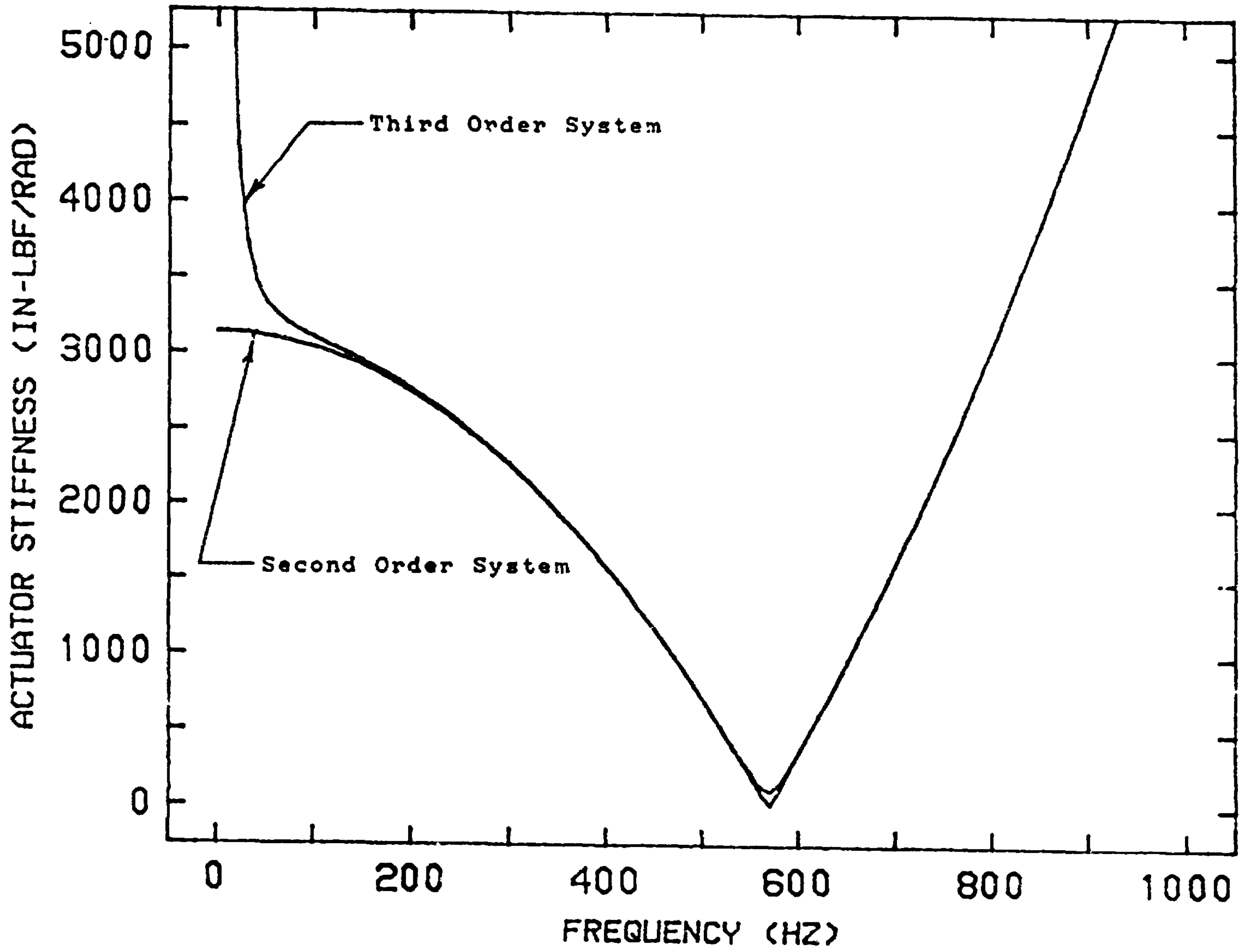

Figure 4–10. AdKEM Large Actuator Dynamic Stiffness for δ = 0.0.

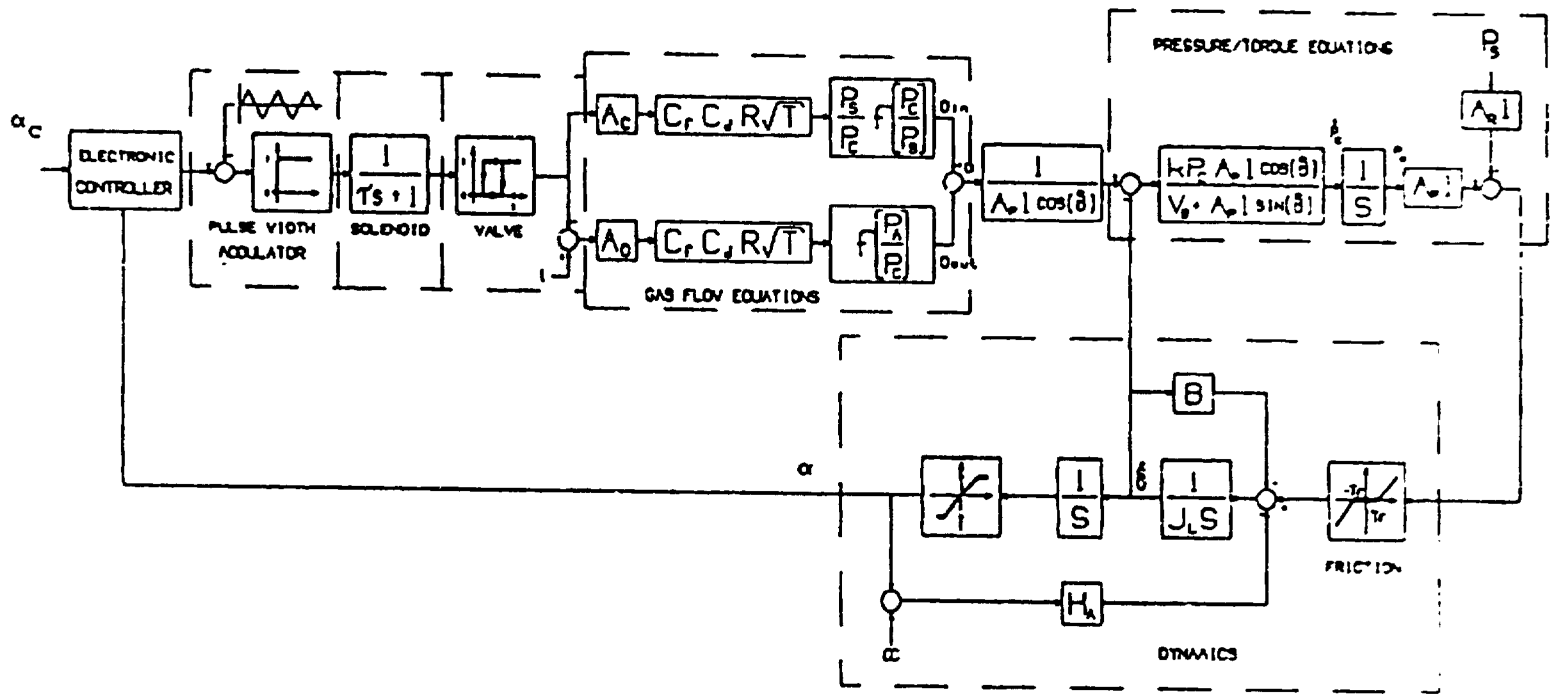

Figure 4–11. <u>Block Diagram of AdKEM Detailed Non–Linear Actuator Model.</u>

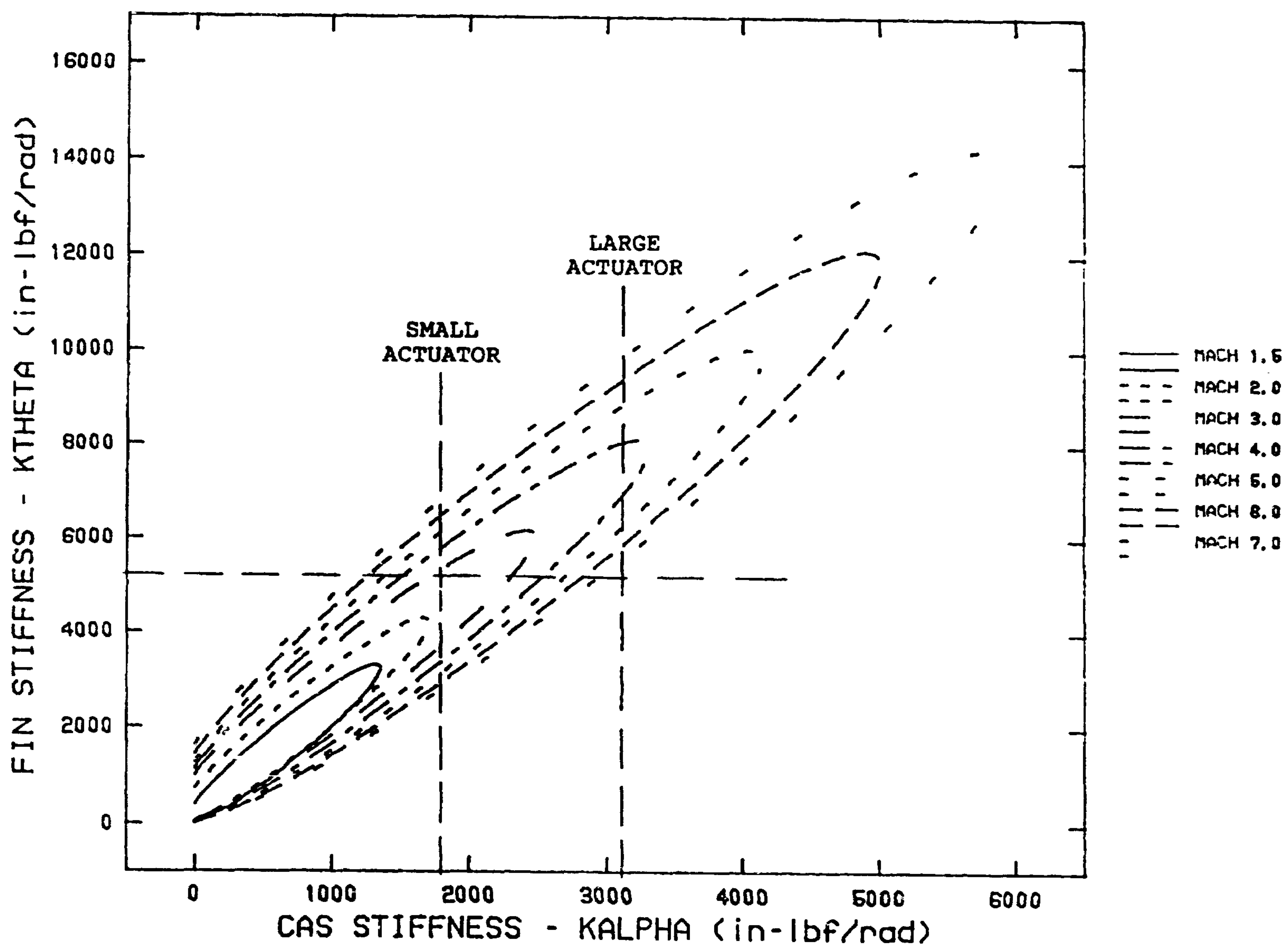

Figure 5–1. Fin Flutter Determination Plot.

NOMENCLATURE

A	Control fin surface area (in^2)
$A(y)$	Control fin root surface area as it varies along the span (in^2)
A_c	Actuator control piston area (in^2)
A_r	Actuator rod area (in^2)
B	Viscous friction coefficient (in–lb_f/rad/s)
$CL\alpha$	Control fin lift coefficient (rad^{-1})
$C\alpha$	Actuator rotational damping factor (in–lb_f–s/rad)
C_θ	Control fin bending damping factor (in–lb_f–s/rad)
E	Modulus of elasticity for steel (lb_f/in^2)
F_L	Lift force (lb_f)
G_c	Actuator compensator gain
$H\alpha$	Hinge moment coefficient (in–lb_f/rad)
I_{xx}	Fin moment of inertia about x–axis (in–lb_f–s^2)
I_{xy}	Fin product of inertia (in–lb_f–s^2)
I_{yy}	Fin moment of inertia about y–axis (in–lb_f–s^2)
K_a	Equivalent actuator valve gain (rad/s/rad)
K_d	Actuator dynamic stiffness factor (in–lb_f/rad)
$K\alpha$	Actuator static stiffness (in–lb_f/rad)
K_θ	Fin bending stiffness factor (in–lb_f/rad)
$K_{\theta s}$	Simplified fin bending stiffness factor (in–lb_f/rad)
L	Actuator lever arm (in)
l_r	Fin root length (in)
l_s	Fin span length (in)
l_t	Fin tip length (in)
$M(y)$	Fin bending moment as it varies along the span (in–lb_f)
Mach	Missile Mach number
n	Specific heat ratio of helium
n_{air}	Specific heat ratio of air
α	Actuator position (rad)

α_{ss}	Actuator steady–state position (rad)
P_{atm}	Atmospheric pressure (psia)
P_c	Actuator control pressure (psia)
P_s	Actuator supply pressure (psia)
Q	Dynamic pressure (psia)
r	Frequency ratio (Ω/Ω_n)
β_{xx}	Aerodynamic viscous damping factor (in^2)
β_{xy}	Aerodynamic viscous damping factor (in^2)
β_{yy}	Aerodynamic viscous damping factor (in^2)
T	Actuator torque output (in–lb_f)
t	Time (s)
T_0	Torque disturbance (in–lb_f)
δ	Damping factor ($C_\alpha \Omega_n / 2K_\alpha$)
θ	Fin bending angle (rad)
Ω	Frequency (rad/s)
$\theta(y)$	Fin slope as it varies along the span (rad)
Ω_n	Natural frequency $(K_\alpha/I_{yy})^{\frac{1}{2}}$ (rad/s)
δy	Numerical integration step size (in)
V	Actuator control chamber volume (in^3)
V_m	Missile velocity (in/s)
V(y)	Fin shear force as it varies along the span (lb_f)
X_{ac}	Location of center of pressure from x–axis (in)
ϕ	Phase angle (rad)
y	Distance along fin span from root (in)
Y_{ac}	Location of center of pressure from y–axis (in)
$z(l_s)$	Fin deflection at tip (in)

REFERENCES

1. Welford, Gordon D., Servo Stiffness of the Second Generation FOG–M Pneumatic Actuator, Technical Report RD–GC–88–20, October 1988.

2. Two Degree of Freedom High Speed Flutter Model and ARAP Simplified Criterion provided by Garrett Fluid Power Systems Division.

APPENDIX A
TWO DEGREE OF FREEDOM HIGH SPEED FLUTTER MODEL and ARAP SIMPLIFIED CRITERION REPORTS

APPENDIX A
TWO DEGREE OF FREEDOM HIGH SPEED FLUTTER MODEL

Consider a fin and coordinate system located at fin center of compliance.

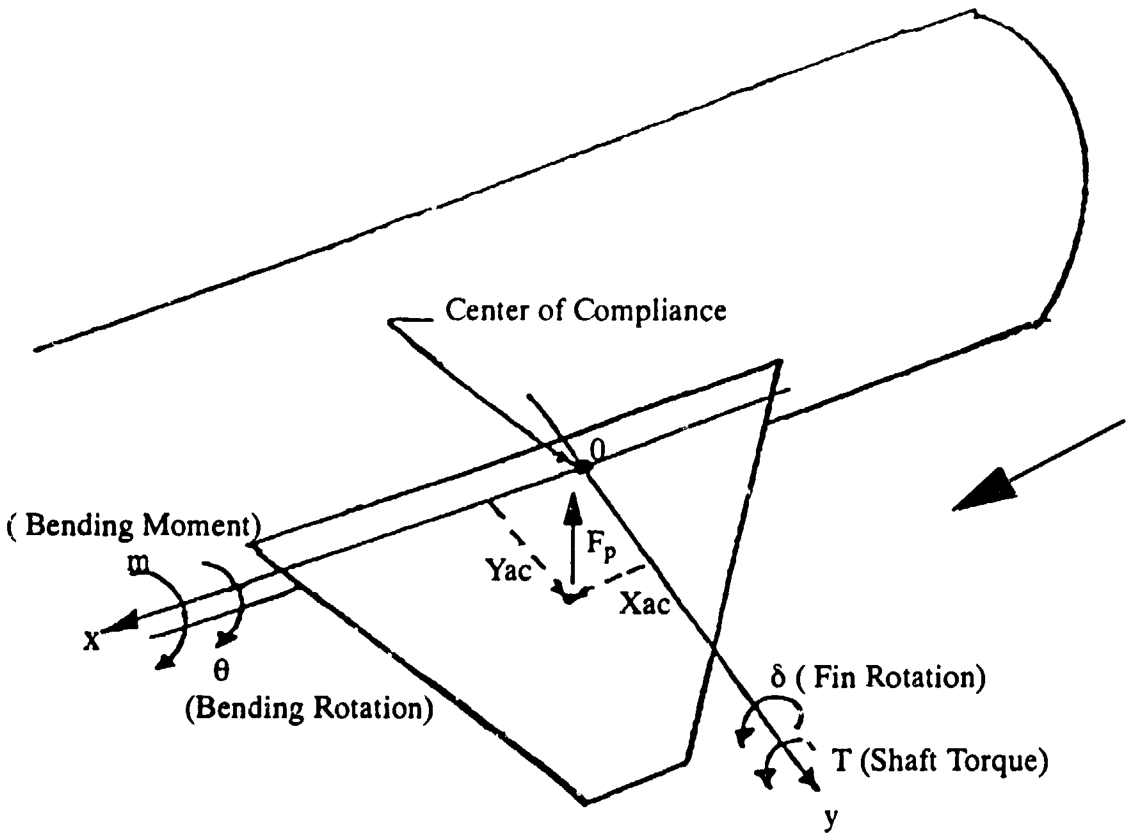

Figure A–1. Sketch of Fin Geometry.

A complete summary of system parameters is presented in Table A–1.
A summary of the dynamic equation of motion is presented in Equation A–1.

TABLE A–1. Description of System Parameters

Parameter	Description	Units
A	Fin surface area	in^2
$C\alpha$	Rotational damping	in–lb–sec/rd
C_θ	Bending damping	in–lb–sec/rd
$CL\alpha$	Panel lift force Coef.	l/rd
F_p	Lift force on panel	lb_f
Ixx	Moment of inertia about x axis	in–lb–sec^2
Iyy	Moment of inertia about y axis	in–lb–sec^2
Ixy	Product of inertia	in–lb–sec^2
K_α	Rotational spring rate	in–lb/rd
K_θ	Bending spring rate	in–lb/rd
M	Bending Moment	in–lbf
Q	Dynamic Pressure ($1/2\rho V^2$)	lb/in^2
T	Shaft Torque.	in–lb
V	Velocity	in/sec
Xac	Dist. of C.P. from x axis	in
Xcg	Dist. of C.G. from x axis	in
Yac	Dist. of C.P. from y axis	in
Ycg	Dist. of C.G. from y axis	in
α	Rotational angle	rd
γ	$I_{xy}/\sqrt{I_{xx}\ I_{yy}}$	1
θ	Bending angle	rd
η_{xx}	Aero viscous damping Coeff.	in^2
η_{xy}	Aero viscous damping Coeff.	in^2
η_{yy}	Aero viscous damping Coeff.	in^2

$$\begin{bmatrix} I_{xx} & I_{xy} \\ I_{xy} & I_{yy} \end{bmatrix} \begin{bmatrix} \ddot{\theta} \\ \ddot{\alpha} \end{bmatrix} + \begin{bmatrix} C_\theta & 0 \\ 0 & C_\alpha \end{bmatrix} \begin{bmatrix} \dot{\theta} \\ \dot{\alpha} \end{bmatrix} + \begin{bmatrix} K_\theta & 0 \\ 0 & K_\alpha \end{bmatrix} \begin{bmatrix} \theta \\ \alpha \end{bmatrix} = \begin{bmatrix} M \\ T \end{bmatrix} \quad \text{(A-1)}$$

The aerodynamic moments presented in Equation A-1 may be expressed by:

$$(-Q/V \ A \ CL_\alpha) \begin{bmatrix} \eta_{yy} & \eta_{xy} \\ \eta_{xy} & \eta_{xx} \end{bmatrix} \begin{bmatrix} \dot{\theta} \\ \dot{\alpha} \end{bmatrix} - (Q \ A \ CL_\alpha) \begin{bmatrix} 0 & Y_{ac} \\ 0 & X_{ac} \end{bmatrix} \begin{bmatrix} \theta \\ \alpha \end{bmatrix} = \begin{bmatrix} M \\ T \end{bmatrix} \quad \text{(A-2)}$$

Equations A-1 and A-2 may be combined to yield:

$$\begin{bmatrix} I_{xx} & I_{xy} \\ I_{xy} & I_{yy} \end{bmatrix} \begin{bmatrix} \ddot{\theta} \\ \ddot{\alpha} \end{bmatrix} + \left\{ \begin{bmatrix} C_\theta & 0 \\ 0 & C_\alpha \end{bmatrix} + (Q/V \ A \ CL_\alpha) \begin{bmatrix} \eta_{yy} & \eta_{xy} \\ \eta_{xy} & \eta_{xx} \end{bmatrix} \right\} \begin{bmatrix} \dot{\theta} \\ \dot{\alpha} \end{bmatrix} +$$
$$\left\{ \begin{bmatrix} K_\theta & 0 \\ 0 & K_\alpha \end{bmatrix} + (Q \ A \ CL_\alpha) \begin{bmatrix} 0 & y_{ac} \\ 0 & x_{ac} \end{bmatrix} \right\} \begin{bmatrix} \theta \\ \alpha \end{bmatrix} = 0 \quad \text{(A-3)}$$

Simplifying Equation A-3 Produces:

$$\begin{bmatrix} I_{xx} & I_{xy} \\ I_{xy} & I_{yy} \end{bmatrix} \begin{bmatrix} \ddot{\theta} \\ \ddot{\alpha} \end{bmatrix} +$$
$$\begin{bmatrix} C_\theta + (Q/V \ A \ CL_\alpha) \ \eta_{yy} & (Q/V \ A \ CL_\alpha) \ \eta_{xy} \\ (Q/V \ A \ CL_\alpha) \ \eta_{xy} & C_\alpha + (Q/V \ A \ CL_\alpha) \ \eta_{xx} \end{bmatrix} \begin{bmatrix} \dot{\theta} \\ \dot{\alpha} \end{bmatrix} +$$
$$\begin{bmatrix} K_\theta & Q \ A \ CL_\alpha Yac \\ 0 & (K_\alpha + Q \ A \ CL_\alpha Xac) \end{bmatrix} \begin{bmatrix} \theta \\ \alpha \end{bmatrix} = 0 \quad \text{(A-4)}$$

Consider solving for the roots of the characteristic equation of expression 4 by taking the Laplace transform of Equation A-4. This expression may then be expressed as:

$$\begin{bmatrix} (I_{xx} \ s^2 + C_{\dot{\theta}} s + K_\theta) & (I_{xy} \ s^2 + C_{\dot{\alpha}\dot{\theta}} s + K_{\alpha\theta}) \\ (I_{xy} \ s^2 + C_{\dot{\alpha}\dot{\theta} s}) & (I_{yy} \ s^2 + C_{\dot{\alpha}} \ s + K_{\alpha\alpha}) \end{bmatrix} \begin{bmatrix} \theta \\ \alpha \end{bmatrix} = 0 \quad \text{(A-5)}$$

Where:

$$C_{\dot{\theta}} = C_\theta + (Q/V \ A \ CL_\alpha) \ \eta_{yy} \quad \text{(A-6a)}$$

$$C_{\dot{\alpha}\dot{\theta}} = (Q/V \ A \ CL_\alpha) \ \eta_{xy} \quad \text{(A-6b)}$$

$$C_{\dot{\alpha}} = C_\alpha + (Q/V \ A \ CL_\alpha) \ \eta_{xx} \quad \text{(A-6c)}$$

$$K_{\alpha\theta} = Q\ A\ Cl_{\alpha} Yac \tag{A-6d}$$

$$K_{\alpha\alpha} = K_{\alpha} + Q\ A\ Cl_{\alpha} Xac \tag{A-6e}$$

The systems characteristic equation is:

$$(Ixx\ s^2 + C_{\theta}\ s + K_{\theta})\ (Iyy\ s^2 + C_{\alpha}\ s + K_{\alpha\alpha}) - (Ixy\ s^2 + C_{\alpha\theta}\ s + K_{\alpha\theta})\ (Ixy\ s^2 + C_{\dot{\alpha}\theta}\ s) = 0$$

Which is also:

$$\begin{aligned}(Ixx\ Iyy - Ixy^2)\ s^4 &+ (Ixx\ C_{\dot{\alpha}} + Iyy\ C_{\dot{\theta}} - 2I_{xy}\ C_{\dot{\alpha}\theta})\ s^3 \\ &+ (Ixx\ K_{\alpha\alpha} + C_{\dot{\theta}}C_{\dot{\alpha}} + Iyy\ K_{\theta} - C_{\dot{\alpha}\dot{\theta}}{}^2 - Ixy\ K_{\alpha\theta})\ s^2 \\ &+ (K_{\alpha\alpha}\ C_{\dot{\theta}} + K_{\theta}C_{\dot{\alpha}} - K_{\alpha\theta}\ C_{\dot{\alpha}\dot{\theta}})\ s + K_{\theta}\ K_{\alpha\alpha} = 0\end{aligned} \tag{A-7}$$

Equation A–7 is the characteristic equation from which the appropriate roots may be computed to determine stability.

The technique for studying flutter consists of finding the flight conditions which generate roots of Equation A–7 with positive real parts. These solutions generate divergent oscillations. A sample solution for a high v flutter problem is found in Figure A–2. This figure shows the boundary between flutter and flutter free operation as a function of rotational springrate, K_{α}, and rotational damping, C_{α}. Note that K_{α} and C_{α} are dominated by actuator springrate and damping. Note also that the flutter boundary is plotted for five values of bending springrate at a constant Mach number and altitude. Figure A–2 illustrates that there are three ways to prevent simple fin flutter.

1. Generate a high value of rotational springrate, K_{α}. For $K_{\alpha} > 8200$ in–lb/rd no combination of conditions can generate flutter.

2. Generate a high value of bending springrate, K_{θ}. For $K_{\theta} > 10000$ in–lb/rd flutter can not occur. There is no value of K_{α} and C_{α} that will generate flutter.

3. Generate sufficient K_{θ} and C_{α} to prevent actuator stiffness and damping characteristics from intersecting the flutter zone. Note a hydraulic damper may be required to achieve sufficient rotational damping in such a scheme.

Note that the technique number one is the traditional solution to fin flutter. However, techniques two and three may be required with a pneumanic fin actuation system.

Figures A–3 and A–4 have been included to show the affect of damping on the flutter boundaries. The analysis of Figure A–3 shows where the flutter boundaries exist when the bending damping, C_{θ}, is reduced to 0. Likewise, Figure A–4 shows the affect of reducing the aerodynamic damping terms to 50% of the value calculated for the specified flight condition.

ARAP SIMPLIFIED CRITERION

A simplified criterion was developed by GPSD and Aeronautical Research Associates of Princeton in order to evaluate K_α and K_θ for flutter free operation. This criterion only applies to highly supersonic fins. A summary of the criterion follows.

If all damping terms are neglected in Equation A–4 then:

$$\begin{bmatrix} Ixx & Ixy \\ Ixy & Iyy \end{bmatrix} \begin{bmatrix} \ddot{\theta} \\ \ddot{\alpha} \end{bmatrix} + \begin{bmatrix} K_\theta & Q\ A\ CL_\alpha\ Yac \\ 0 & (K_\alpha + Q\ A\ CL_\alpha\ Xac) \end{bmatrix} \begin{bmatrix} \theta \\ \alpha \end{bmatrix} = 0 \qquad \text{(A–8)}$$

Likewise the system characteristic equation becomes:

$$(Ixx\ Iyy - Ixy^2)\ s^4 + (Ixx\ K_{\alpha\alpha} + Iyy\ K_\theta - Ixy\ K_{\alpha\theta})\ s^2 + K_{\alpha\alpha}\ K_\theta = 0 \qquad \text{(A–9)}$$

If the characteristic equation is factored, the condition where all four roots have the same frequency (that is the condition where flutter begins) is:

$$\begin{aligned} (Ixx\ K_{\alpha\alpha}) - 2\ Ixx\ Iyy\ K_{\alpha\alpha}\ K_\theta - 2\ Ixx\ Ixy\ K_{\alpha\alpha}\ K_{\alpha\theta} \\ - 2\ Iyy\ Ixy\ K_\theta\ K_{\alpha\theta} + (Iyy\ K_\theta)^2 + (Ixy\ K_{\alpha\theta})^2 \\ + 4\ Ixy^2\ K_\theta\ K_{\alpha\alpha} = 0 \end{aligned} \qquad \text{(A–10)}$$

Equation A–10 which is the boundary of flutter is plotted for the sample case in Figure A–5. In this figure the fin flutter boundary is presented as a function of rotational and bending stiffness. Of particular interest are points A and B on this curve. If bending stiffness, K_θ, is greater than that defined by point A then no flutter can occur. If rotational stiffness, K_α, is greater than that defined by point B, then no flutter can occur. Points A and B are defined by:

Point A $K_\theta \geq Ixx/Ixy\ Q\ A\ CL_\alpha\ Yac$
(No Flutter) (A–11a)

Point B $K_\alpha \geq Iyy/Ixy\ Q\ A\ CL_\alpha\ Xac - Q\ A\ CL_\alpha\ Xac$
(No Flutter) (A–11b)

Refering to Figures A–2, A–3, A–4, and A–5, the following conclusions may be reached:

1. Figure A–2 illustrates that increasing C_α can increase the value of K_α that is required for absolute stability. Figures A–3 and A–4 illustrates that decreasing either bending damping or aerodynamic damping will increase the rotational stiffness necessary for absolute stability (Point B).

2. The analysis of Figures A–2, A–3, and A–4 shows that the criterion for the bending springrate required for absolute stability, (Point A), is affected only slightly by system

damping. The bending stiffness requirement, for absolute stability, that is predicted assuming zero damping is 9650 in–lb/rd. Variations in the damping terms increased this figure only slightly to 10,000 in–lb/rd.

The simple criterion described above can therefore be used as a useful guide to predict the bending stiffness, K_θ, that can be used to eliminate flutter regardless of the values of rotational stiffness, K_α, and rotational damping, C_α.

A more detailed analysis is required to predict the rotational stiffness, K_α, that is required to produce absolute stability because of the significant affects of system damping on the flutter boundaries. Using such an approach to eliminate flutter is therefore much more involved and may require controlling both rotational stiffness, K_α, and damping, C_α.

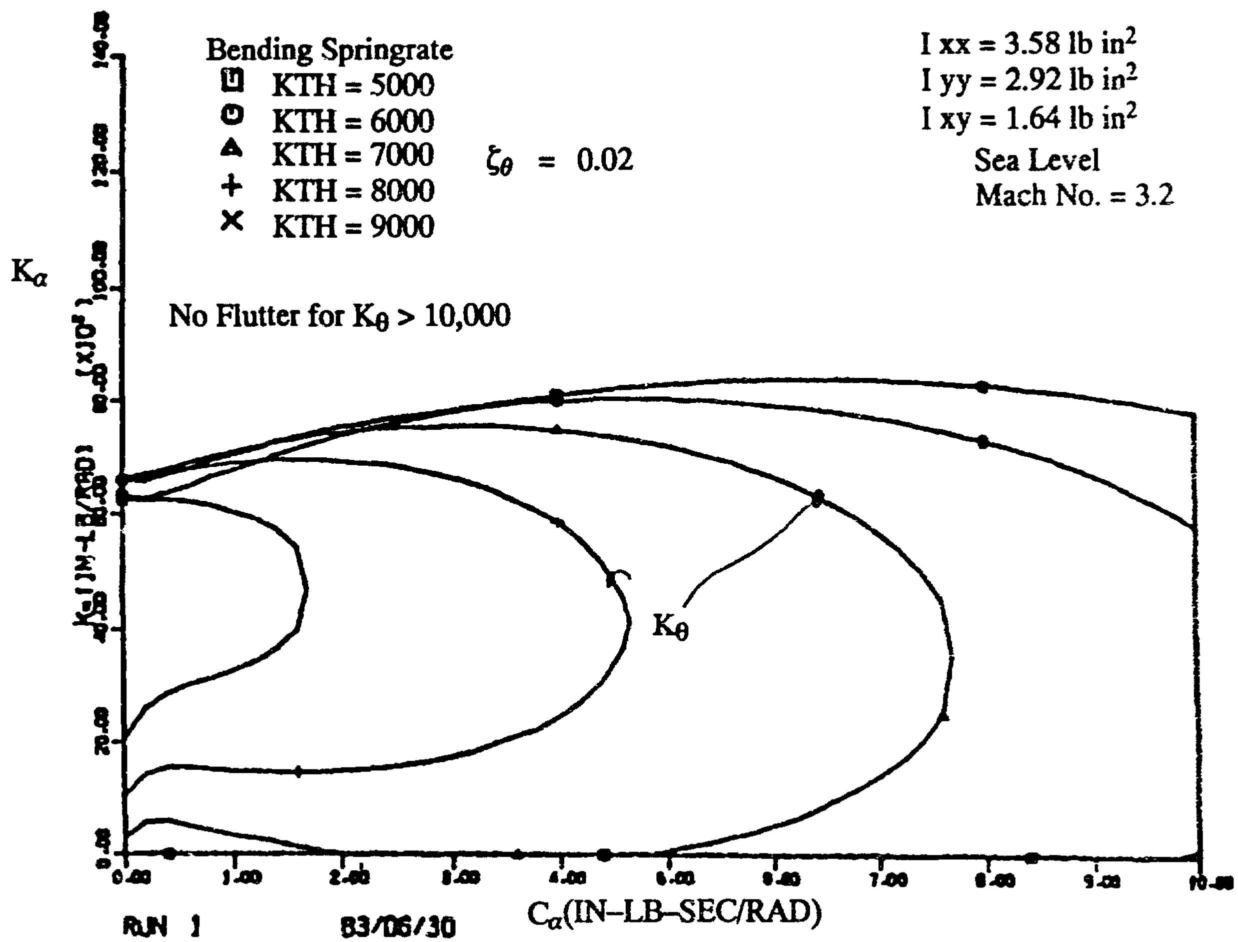

Figure A–2. Sample Flutter Boundaries for High δ Fin.

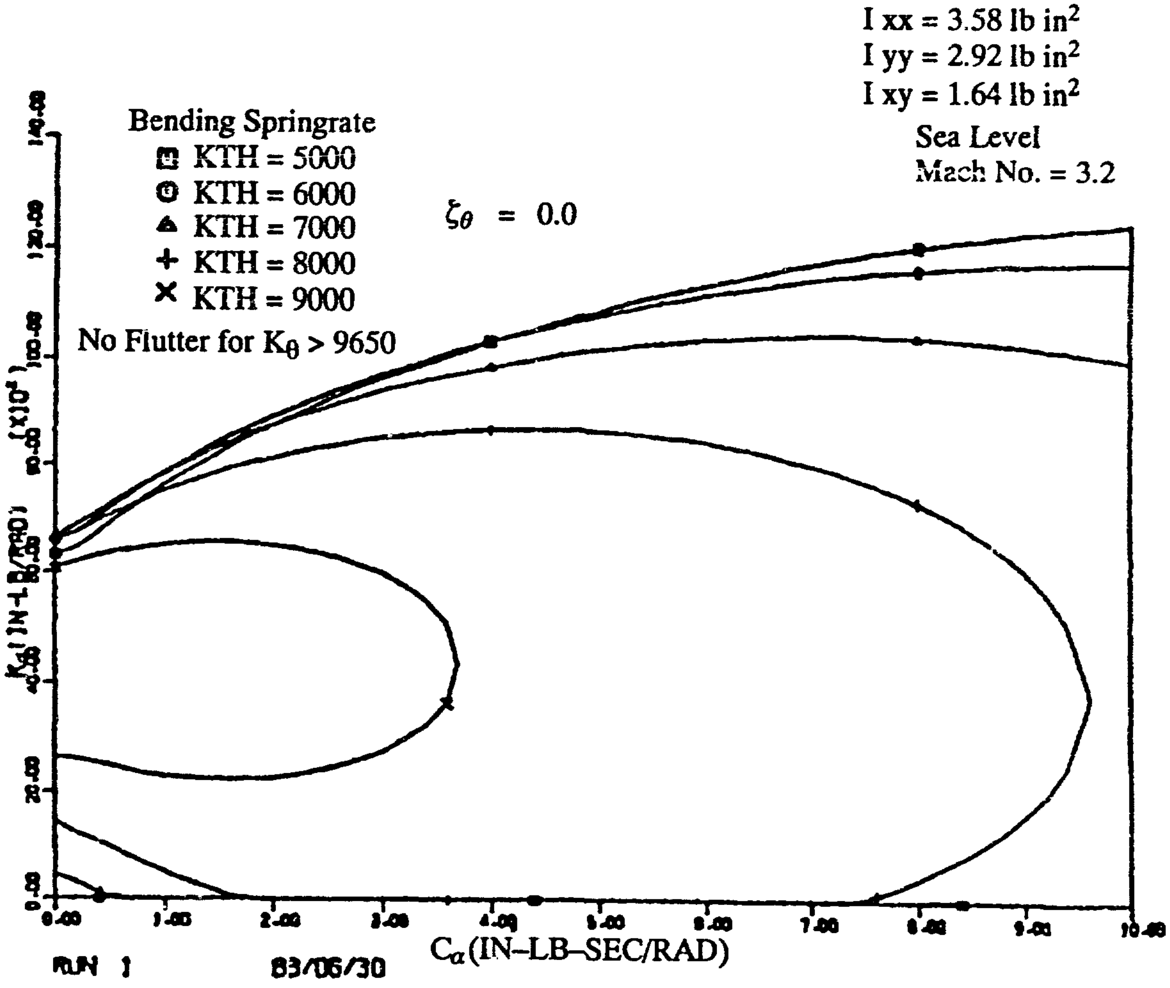

Figure A–3. Sample Flutter Boundaries for High δ Fin.

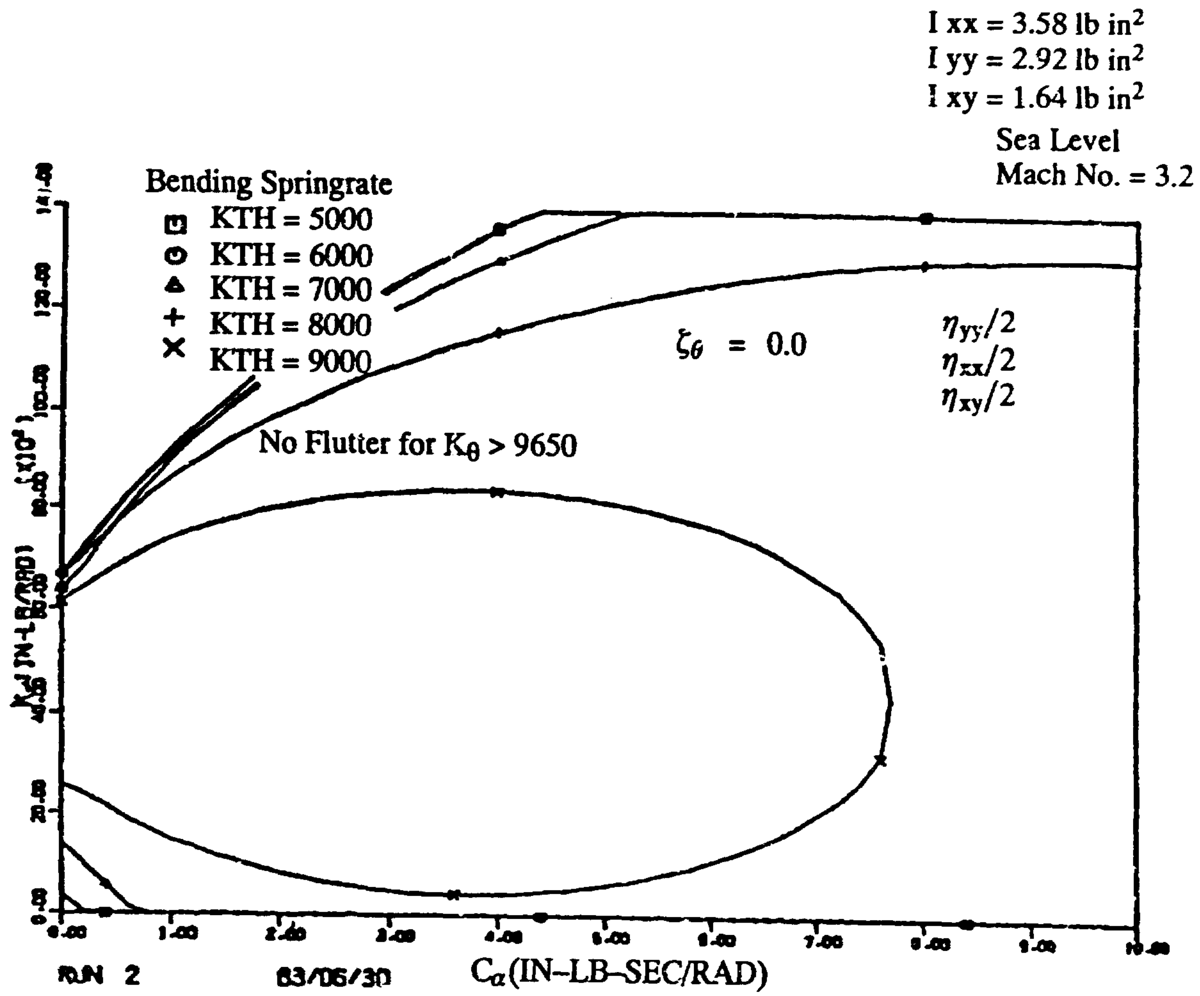

Figure A–4. Sample Flutter Boundaries for High δ Fin.

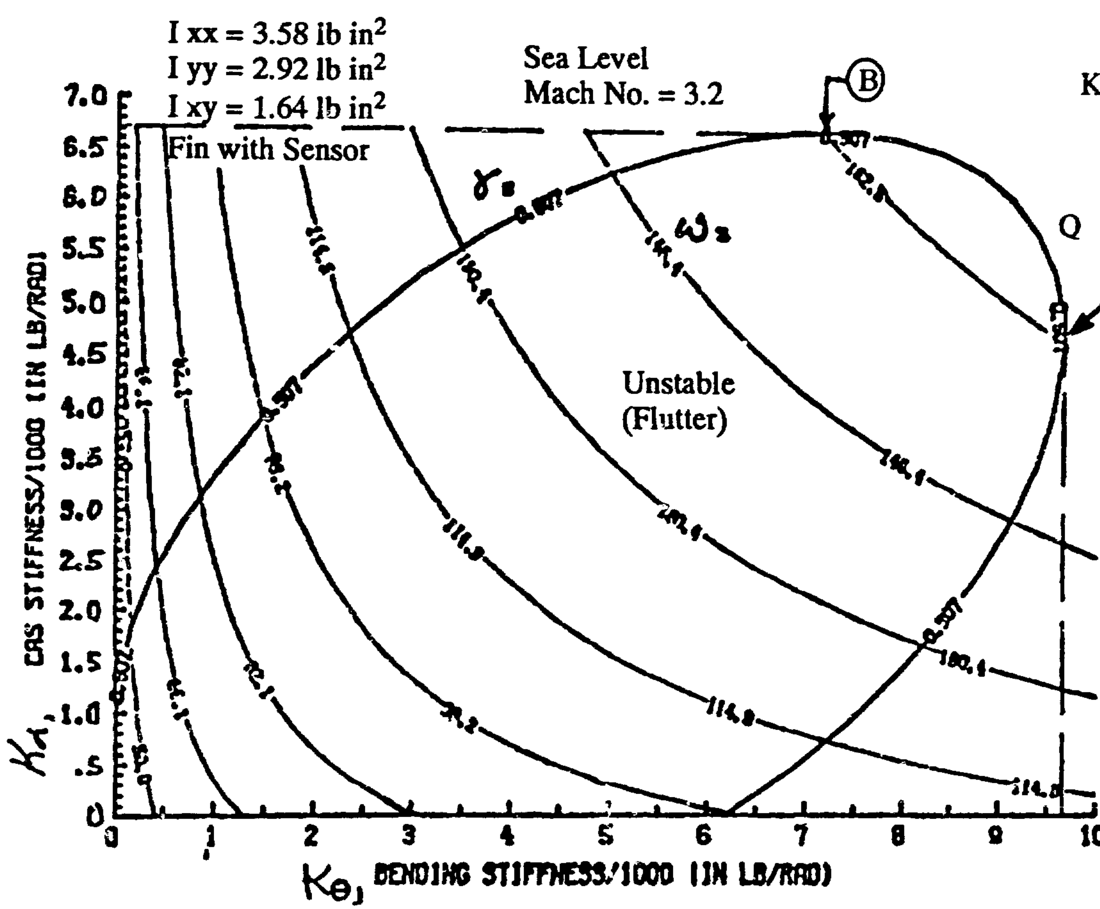

$$= 6700$$

$$K_\alpha = \frac{Iyy}{Ixy} \; Q \; A \; CL_\alpha \; Yac - Q \; A \; CL_\alpha \; X\alpha c$$

$$Q \; A \; CL_\alpha X\alpha c = 1170.95$$

$$K_\theta = \frac{Ixx}{Ixy} \; Q \; A \; CL_\alpha \; Y_\alpha$$

$$= 9650$$

$$Q \; A \; CL_\alpha \; Yc = 4420.67$$

Figure A–5. Sample ARAP Flutter Boundary.

APPENDIX B

STABILITY EQUATION PROGRAM LISTING

```
C    PROGRAM NAME: FINSIMP FOR

C    Steve Cayson

C    US Army Missile Command
C    Research, Development, and Engineering Center
C    Redstone Arsenal, AL
C    OCT-NOV 89

C    This program is used to calculate the flutter regions for the
C    AdKEM control section fin using equations developed in a paper
C    written by Garrett Fluid Systems Division in Phoenix, AZ. The
C    equations were developed using a two-degree-of-freedom model for
C     a control surface assuming no damping terms. The characteristic
C    equation for this system was then found and used to calculate the
C    fin stabilty regions based on fin and actuator stiffness and
C    aerodynamic parameters. The region is solved for and the data is
C    written to a file, FLUTTER.DAT, that can be plotted.

C    VARIABLE     DESCRIPTION

C    IXX          Fin inertia about hinge line (in-lbf-s^2)
C    IYY          Fin inertia about root line (in-lbf-s^2)
C    IXY          Fin product of inertia (in-lbf-s^2)
C    REFA         Control fin surface area (in^2)
C    Q            Dynamic pressure (psia)
C    MACH         Mach number
C    V            Missile velocity (in)
C    CLIFT        Fin lift coefficient (rad^-1)
C    XCP          Distance of center of pressure from x-axis (in)
C    YCP          Distance of center of pressure from y-axis (in)
C    KALPHA       Fin bending stiffness factor (in-lbf/rad)

       REAL IXX, IYY, IXY, KAA, KAT, KALPHA, KTHETA, MACH

       DIMENSION A(11), B(11), C(26), D(26), E(25), F(25)

       DIMENSION RR(10), RI(10) ,AA(26), BB(26), RREAL(25), RIMAG(25)

       OPEN(4, FILE='FLUTTER.DAT' ,STATUS='NEW')

C    ***** CONSTANTS USED IN ROOT SOLVER SUBROUTINE *****

C    - ORDER OF POLYNOMIAL EQUATION
       NN = 2
```

```
C   - INITIAL ESTIMATES FOR ROOTS
        X0 = 5.
        Y0 = 5.
        X  = X0
        Y  = Y0

C   ***** INPUT FIN CHARACTERISTICS *****

C   - INERTIAS (in-lbf-s^2)
        IXX =  .00028543
        IYY =  .00012277
        IXY =  .000028672

C   - FIN REFERENCE AREA (in^2)
        REFA = 3.463

C   - INPUT MACH NUMBER AND CALCULATE DYNAMIC PRESSURE (psia)
        WRITE(*, 100)
  100   FORMAT(2X, 'MACH NUMBER?',2X)
        READ (*, 110)MACH
  110   FORMAT( F10.7)

        Q = 10.29* (MACH**2.)

C   - CALCULATE LOCAL VELOCITY (in/s) ASSUMING TEMP 70F
        V = MACH*13540.

C   - INPUT FIN LIFT COEFFICIENT (rad^-1) AND CP (in) AT MACH NUMBER
        WRITE(*, 120)MACH
  120   FORMAT(/,2X,'LIFT COEFFICIENT AT MACH ', F5.2,' ? (1/rad)', 2X)
        READ(*, 110) CLIFT
        WRITE(*, 130)
  130   FORMAT(/, 2X, 'DIST OF CP FROM HINGE LINE (+ is in aft direction)'
     &,    2X)
        READ(*, 110)XCP
        YCP = 0.91

C   ***** LOOP TO DETERMINE FLUTTER REGION *****
      DO 200 K = 0, 10000, 20
        KALPHA = K*1.0

C   - PRELIMINARY CALCULATIONS
        QUANT = Q*REFA*CLIFT
        KAT = QUANT*YCP
        KAA = KALPHA + QUANT*XCP

C   - REAL COEFFICIENTS OF POLYNOMIAL - A(1) IS HIGHEST ORDER COEF.
        A(1) = IYY**2.
        A(2) = 4*KAA*(IXY**2.) - 2*IYY*IXY*KAT - 2*IXX*IYY*KAA
        A(3) = (IXX*IXX*KAA*KAA) + (IXY*KAT)**2. - 2*IXX*IXY*KAA*KAT
```

```
C    - IMAGINARY COEFFICIENTS OF POLYNOMIAL
           B(1) = 0.
           B(2) = 0.
           B(3) = 0.

C    - SOLVE FOR ROOTS USING SUBROUTINE ROOTS
           CALL ROOTS(A, B, NN, X, Y, RR, RI, NERR)

C    - CHECK TO SEE IF ROOTS ARE EQUAL, IF SO HALT PROGRAM EXECUTION
           CHECK = RR(1) - RR(2)
           IF (ABS(CHECK) .LT.  .1) GOTO 99

           IF (RR(1) .LT. 0.0) RR(1) = 0.0
           IF (RR(2) .LT. 0.0) RR(2) = 0.0

C          WRITE(*,10)  KALPHA, RR(1), RR(2)
           WRITE(4, 10)  KALPHA, RR(1), RR(2)
   10  FORMAT(2X, F7.1, 2(2X, F10.3))
  200  CONTINUE
   99  END


SUBROUTINE ROOTS(A, B, NN, X0, Y0, RR, RI, NERR)
DOUBLE PRECISION AA, BB, RREAL,  RIMAG, C, D, E, F, P, Q, X, Y, TOL, DENOM,
R, RS
DIMENSION A(*), B(*), RR(*), RI(*)
DIMENSION AA(26), BB(26), C(26), D(26)
DIMENSION RREAL(25), RIMAG(25), E(25), F(25)
C         INITIALIZE
      NERR = 0
      R = 0.0D0
      N = NN
      NP1 = N+1
      K = 0
      TOL = .5D-8
      X = X0
      Y = Y0
      DO 5  I=1, NP1
      AA(I) = A(I)
    5 BB(I) = B(I)
C         TEST FOR FIRST DEGREE EQUATION
   10 IF(N .EQ. 1)  GOTO 60
C         BEGIN SYNTHETIC DIVISION FOR F(Z)  AND F'(Z)
   20 KTR = 0
      NP1 = N+1
      IF(X  .EQ. 0.0D0)  X=.37D0
      IF(Y  .EQ. 0.0D0)  Y=.37D0
      C(1) = AA(1)
      D(1) = BB(1)
      E(1) = C(1)
```

```
      F(1) = D(1)
   23 DO 25 I=2,NP1
      IM1 = I-1
      C(I) = AA(I) + X*C(IM1) - Y*D(IM1)
      D(I) = BB(I) + Y*C(IM1) + X*D(IM1)
      IF(I .EQ. NP1) GOTO 25
      E(I) = C(I) + X*E(IM1) - Y*F(IM1)
      F(I) = D(I) + Y*E(IM1) + X*F(IM1)
   25 CONTINUE
C        CALCULATE X AND IY
   30 DENOM = E(N)**2+F(N)**2
      P = (C(NP1)*E(N) + D(NP1)*F(N))/DENOM
      Q = (D(NP1)*E(N) - C(NP1)*F(N))/DENOM
      X = X-P
      Y = Y-Q
      RS = R
      R = DSQRT(P**2+Q**2)
      IF(R .LT. RS) GOTO 40
C        TEST LOOP COUNTER WHEN CORRECTION DOES NOT DECREASE
      KTR = KTR+1
      IF(KTR .LE. 25) GOTO 40
      NERR = 1 GOTO 50
C        CHECK FOR CONVERGENCE
   40 IF(R .GT. TOL) GOTO 23
C        ROOT FOUND - REDUCE POLYNOMIAL
   50 K = K+1
      RREAL(K) = X
      RIMAG(K) = Y
      DO 55 I=1, N
      AA(I) = C(I)
   55 BB(I) = D(I)
      N = N-1
      GOTO 10
C        SOLUTION FOR FIRST DEGREE POLYNOMIAL
   60 DENOM = AA(1)**2+BB(1)**2
      x = (-AA(1)*AA(2) - BB(1)*BB(2))/DENOM
      Y = ( AA(2)*BB(1) - AA(1)*BB(2))/DENOM
      K = K+1
      RREAL(K) = X
      RIMAG(K) = Y
C        MOVE DOUBLE PRECISION ROOTS TO SINGLE PRECISION OUTPUT
   70 DO 75 I=1,NN
      RR(I) = RREAL(I)
   75 RI(I) = RIMAG(I)
C
  999 RETURN
      END
```

APPENDIX C

FIN MOMENT OF INERTIA EQUATIONS DEVELOPMENT

APPENDIX C

The leading wedge of the control fin root is represented as shown in Figure 3–2. The width, $b_3(y)$, is calculated using

$$b_3(y) = (l_{t3} - l_{r3})(y/l_s) + l_{r3} \quad \text{(C–1)}$$

and the thickness, $t_3(y)$, is found from the equation

$$t_3(y) = (t_s - t_r)(y/l_s) + t_r \quad \text{(C–2)}$$

The leading edge thickness can be calculated using

$$t_{le}(y) = (t_{sle} - t_{rle})(y/l_s) + t_{rle} \quad \text{(C–3)}$$

A trapezoid such as the one shown below has now been defined and the inertia about the x–axis can be found.

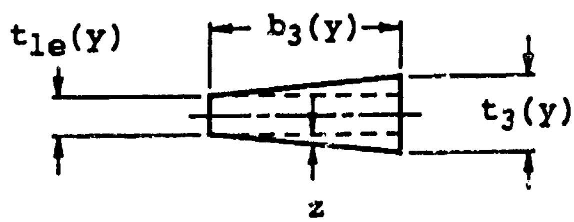

Figure C–1. Typical Fin Wedge Cross–Section

The trapezoid may be divided into two regions, the rectangular portion and the triangular portion. The inertia of the rectangular portion is just

$$I_{3R}(y) = [b_3(y)\, t_{le}(y)^3]/12 \quad \text{(C–4)}$$

The inertia of the triangular sections can be found by integration of

$$I_{3T} = 2\int_A z^2 \, dA \quad \text{(C–5)}$$

where z is the distance as shown in Figure C–1. Substitution of the proper limits into Equation C–5 results in the double integral

$$I_{3T} = 2\int_0^{b_3(Y)} \int_{b_{z3}}^{m_{z3}x+b_{z3}} z^2 \, dz\, dx \quad \text{(C–6)}$$

where

$$b_{z3} = t_{le}(y)/2 \tag{C-7}$$

and

$$m_{z3} = [t_3(y) - t_{le}(y)]/[2\, b_3(y)] \tag{C-8}$$

Evaluation of Equation C–6 results in

$$I_{3T}(y) = b_3(y)^2 \{m_{z3}{}^3 b_3(y)^2/6 + 2m_{z3}{}^2 b_{z3} b_3(y)/3 + m_{z3} b_{z3}{}^2] \tag{C-9}$$

and the total inertia of the leading wedge section as a function of y is

$$I_3(y) = I_{3R}(y) + I_{3T}(y) \tag{C-10}$$

The inertia of the trailing section is found similarly. The inertia of the rectangular portion is

$$I_{1R}(y) = [b_1(y)\, t_{te}(y)^3]/12 \tag{C-11}$$

and the inertial of the triangular section is

$$I_{1T}(y) = [b_1(y)^2\, [m_{z1}{}^3 b_1(y)^2/6 + 2m_{z1}{}^2 b_{z1} b_1(y)/3 + m_{z1} b_{z1}{}^2] \tag{C-12}$$

where

$$b_1(y) = (l_{tl} - l_{rl})(y/l_S) + 1_{rl} \tag{C-13}$$

$$t_1(y) = (t_S - t_r)(y/l_S) + t_r \tag{C-14}$$

$$t_{te}(y) = (t_{ste} - t_{rte})\,(y/l_S) + t_{rte} \tag{C-15}$$

$$b_{zl} = t_{te}(y)/2 \tag{C-16}$$

$$m_{zl} = [t_1(y) - t_{te}(y)]/[2\, b_1(y)] \tag{C-17}$$

Therefore, the total inertia of the trailing wedge is

$$I_1(y) = I_{1R}(y) + I_{1T}(y) \tag{C-18}$$

The middle section of the fin is simply a rectangle and the inertia is found using

$$I_2(y) = b_2(y)\, t_2(y)^3/12 \tag{C-19}$$

where

$$h_2(y) = (l_{t2} - l_{r2})\,(y/l_S) + l_{r2} \qquad \text{(C–20)}$$

and

$$t_2(y) = (t_s - t_r)\,(y/l_S) + t_r \qquad \text{(C–21)}$$

The total inertia of the section is then found from

$$I_{tot}(y) = I_1(y) + I_2(y) + I_3(y) \qquad \text{(C–22)}$$

APPENDIX D

BENDING PROGRAM LISTING

```
C    PROGRAM NAME: FULLFIN.FOR

C    Steve Cayson
C    US Army Missile Command
C    Research, Development, and Engineering Center
C    Control Systems Branch
C    04 DEC 89

C    This program will calculate the fin bending spring rate for the
C    stainless steel core of the AdKEM control fin assuming a constant
C    distributed load (dynamic pressure) on the fin. First of all the
C    fin geometry is input to the program. This includes the span,
C    various thicknesses, and the root and tip lengths. Then a
C    loop is used to calculate the moment and slope at each point along
C    the span and solve for the stiffness measured in in-lbf/rad.
C    The equation is
C
C           K(Y) = dMOMENT/dTHETA

C    VARIABLE    DESCRIPTION

C    THKFACT     Thickness multiplier for variable thicknesses
C    LR1         Trailing wedge length at root (in)
C    LR2         Mid-section length at root (in)
C    LR3         Leading wedge length at root (in)
C    LRTOT       Total fin length at root (in)
C    TROOT       Mid-section thickness at root (in)
C    LT1         Trailing wedge length at tip (in)
C    LT2         Mid-section length at tip (in)
C    LT3         Leading wedge length at tip (in)
C    LTTOT       Total fin tip length (in)
C    TSPAN       Mid-section thickness at span (in)
C    LSPAN       Length of span (in)
C    TSLE        Thickness of leading edge at span (in)
C    TRLE        Thickness of leading at root (in)
C    TSTE        Thickness of trailing edge at span (in)
C    TRTE        Thickness of trailing edge at root (in)
C    ATOT        Total fin root area (in2)
C    MOM1        Bending moment at fin root (in-lbf)

      IMPLICIT REAL (I ,K-M)
      DOUBLE PRECISION THETA1, THETA2, DELTHT, XDEF, DY
      OPEN(4, FILE='FULL.DAT', STATUS = 'NEW')
      THKFACT = 1.0

C    ***** INPUT FIN GEOMETRY SPECIFICATIONS *****
```

```
C   ROOT GEOMETRY (ALL DIMENSIONS IN INCHES)
         LR1 = .699
         LR2 = .822
         LR3 = .674
         LRTOT = LR1 + LR2 + LR3
         TROOT = THKFACT * 0.1

C   TIP GEOMETRY
         LT1 = .299
         LT2 = .444
         LT3 = .357
         LTTOT = LT1 + LT2 + LT3
         TSPAN = THKFACT * 0.057

C   SPAN LENGTH
         LSPAN = 1.80

C   LEADING AND TRAILING EDGE THICKNESSES AT ROOT AND SPAN
         TSLE = THKFACT * .017
         TRLE = THKFACT * .025
         TSTE = THKFACT * .025
         TRTE = THKFACT * .025

C   CALCULATE TOTAL FIN AREA AND BENDING MOMENT AT Y=0
         ATOT = LSPAN/2. * (LRTOT + LTTOT)
         MOM1 = LSPAN/6. * (LSPAN*(LTTOT + 2.*LRTOT) - 6.*ATOT)

C   ***** OTHER VARIABLES *****
C   FIN COEFFICIENT OF ELASTICITY (psi)
         E = 28.5E06
C   INTEGRATION STEP SIZE
         DY = .001
C   DO LOOP TERMINATION VALUE CALCULATION
         JDY = LSPAN/DY
C   LOOP INITIALIZATION
         SUMMOI = .0
         THETA1 = .0
         ZDEF = .0
         JPRINT = 1

C   !!!!!!!!!!!!!!!!!!!!!!!!!!!!!!!!!!!!!!!!!!!!!!!!!!!!!!!!!!!!!!!!!!!!!!!!!!!!!!!!!!!!!!!!!!
C   !!!!!!!!!!!!!!!!!!!!DON'T MESS WITH ANYTHING BELOW HERE!!!!!!!!!!!!!!!!!!!
C   !!!!!!!!!!!!!!!!!!!!!!!!!!!!!!!!!!!!!!!!!!!!!!!!!!!!!!!!!!!!!!!!!!!!!!!!!!!!!!!!!!!!!!!!!!

C   ***** BEGIN NUMERICAL INTEGRATION TO SOLVE FOR STIFFNESS *****
         DO 10 J = 1, JDY-9
         Y = J*DY

C   ***** CALCULATE CROSS-SECTIONAL INERTIA OF FIN AT Y *****
C   CALCULATE TRAILING SECTION PARAMETERS
```

```
      B1 = (LT1-LR1)*Y/LSPAN + LR1
      T1 = (TSPAN-TROOT)*Y/LSPAN + TROOT
      TTE = (TSTE-TRTE)*Y/LSPAN + TRTE
      MZ1 = (T1-TTE)/(2.*B1)
      BZ1 = TTE/2.

C   CALCULATE TRAILING SECTION INERTIA
C   (RECTANGULAR PORTION)
      XI1R = (1/12.)*B1*(TTE**3)
C   (TRIANGULAR PORTION)

XI1T = B1*( ( (MZ1*B1)**3)/6. + (2.*BZ1/3. )*(MZ1*B1)**2 +
    &        MZ1*B1*BZ1**2)
C   TOTAL
      XI1 = XI1R + XI1T

C   CALCULATE MIDDLE SECTION INERTIA
      C1 = (LT2-LR2)*Y/LSPAN + LR2
      C2 = ((TSPAN-TROOT)*Y/LSPAN + TROOT)**3
      C3 = 1/12. XI2 = C3*C1*C2

C   CALCULATE LEADING SECTION PARAMETERS
      B3 = (LT3-LR3)*Y/LSPAN + LR3
      T3 = (TSPAN-TROOT)*Y/LSPAN + TROOT
      TLE = (TSLE-TRLE)*Y/LSPAN + TRLE
      MZ3 = (T3-TLE)/(2.*B3)
      BZ3 = TLE/2.

C   CALCULATE LEADING SECTION INERTIA
C   (RECTANGULAR PORTION)
      XI3R = (1/12.)*B3*(TLE**3)
C (TRIANGULAR PORTION)
      XI3T = B3*(((MZ3*B3)**3)/6. + (2.*BZ3/3.)*(MZ3*B3)**2 +
    &        MZ3*B3*BZ3**2)
C   TOTAL
      XI3 = XI3R + XI3T
C   TOTAL INERTIA OF CROSS-SECTION
      XITOT = XI1 + XI2 + XI3
C   ***** CALCULATE BENDING STIFFNESS *****
C   CALCULATE MOMENT/DYNAMIC PRESSURE AT Y AND CHANGE IN
      MOMENT M0M2 = ATOT*(Y-LSPAN) - LRTOT/2.*(Y**2.-LSPAN**2.) -
    &   (LTTOT-LRTOT)*(Y**3.-LSPAN**3.)/(6.*LSPAN)
      DELMOM = MOM2 - MOM1
C   CALCALUTE THETA/DYNAMIC PRESSURE AT Y AND CHANGE IN THETA
      RAT = MOM2/XITOT
      SUMMOI = SUMMOI + (MOM2/XITOT)*DY
      THETA2 = SUMMOI/E
      DELTHT = THETA2 - THETA1
```

```
C    CALCULATE DEFLECTION/DYNAMIC PRESSURE
          ZDEF = ZDEF + THETA2*DY

C    CALCULATE FIN STIFFNESS
          KFINY = ABS(DELMOM DELTHT)

MOM1 = MOM2 THETA1 = THETA2

C    ***** WRITE DATA TO FILE *****
C    PRINT EVERY 10th DATA POINT
          IF (JPRINT .EQ. 10) THEN

C    WRITE SPRING RATE AT Y TO FILE
          WR1TE(4, 100)Y, KFINY, MOM2, THETA2, ZDEF
 100     FORMAT(2X, F6.4, 2X, E15.3, 2X, F11.3, 2X, E15.3, 2X, E15.3)

          JPRINT = 0
       ENDIF

       JPRINT = JPRINT+1

 10    CONTINUE

       END
```

DISTRIBUTION LIST

		copies
AMSMI-RD		1
AMSMI-RD-CS-R		15
AMSMI-RD-CS-T		1
AMSMI-GC-IP,	Mr. Fred M. Bush	1
U. S. Army Materiel System Analysis Activity ATTN: AMXSY-MP (Herbert Cohen) Aberdeen Proving Ground, MD 21005		1
IIT Research Institute ATTN: GACIAC 10 W. 35th Street Chicago, IL 60616		1
AMSMI-RD-GC,	Mr. Sliz	1
AMSMI-RD-GC-C,	Mr. Warren	1
	Mr. Dunaway	1
	Mr. Dixon	1
	Mr. Berry	10
	Mr. Cayson	10
	Ms. Butler	1
AMSMI-RD-ST-WF,	Mr. Schexnayder	1
	Col Price	1
AMSMI-RD-ST-SA,	Mr. Christensen	1
	Mr. Schaeffel	1
	Mr. Nourse	1
	Mr. Hall	1
ASMI-RD-SS-AT,	Mr. Washington	1
	Mr. Ferguson	1